

INTC-P-495  
CERN-INTC-2017-012

# Shell structure of odd neutron-rich $^{71-75}\text{Cu}$ isotopes via one proton transfer reactions



Spokespersons:                    Oleksii Poleshchuk  
    Riccardo Raabe

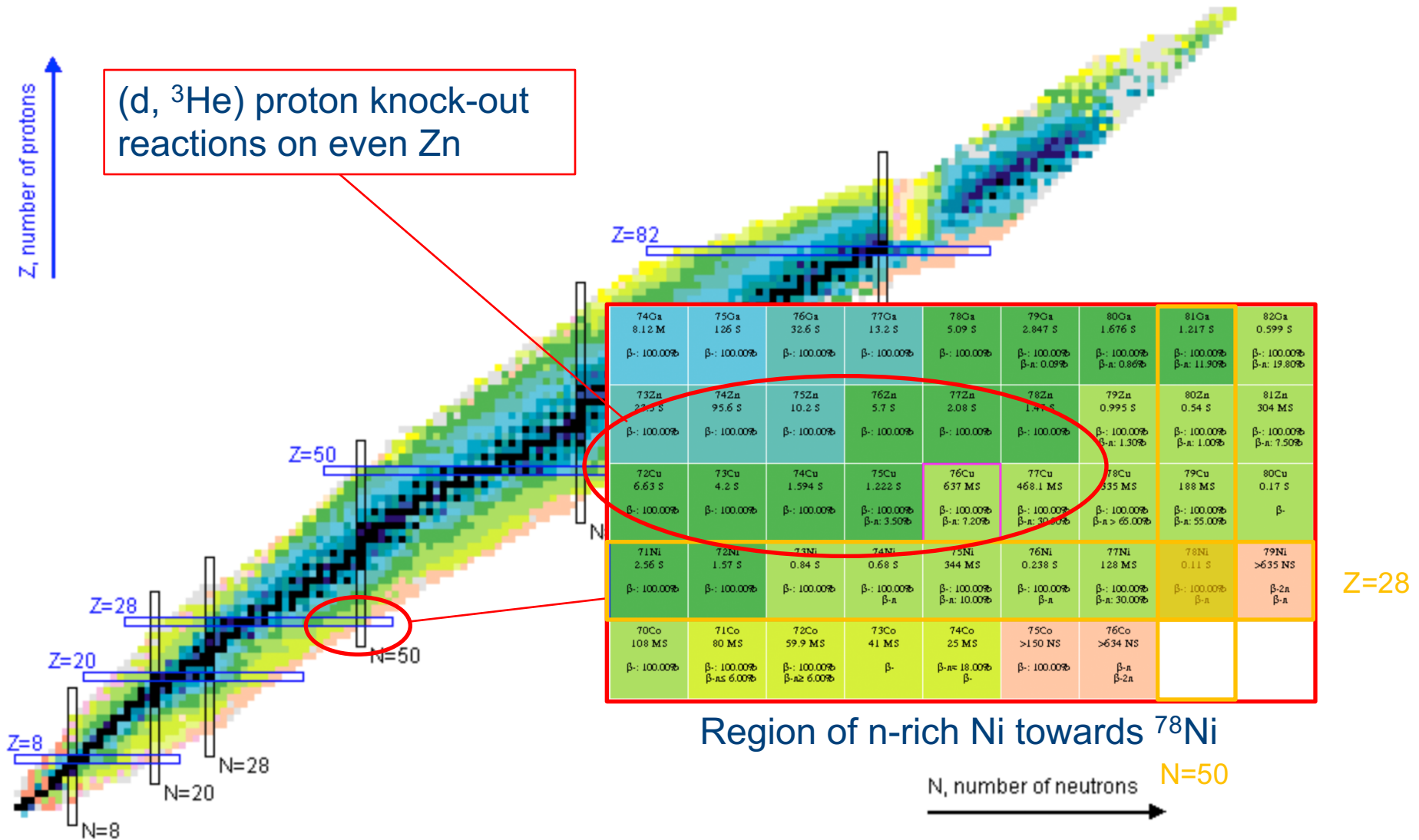
Contact person:                    Liam Gaffney

ISOLDE and Neutron Time-of-Flight Experiments Committee

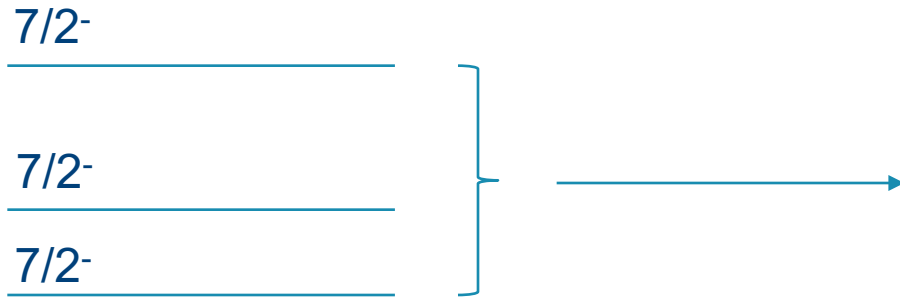
February 8<sup>th</sup>, 2017



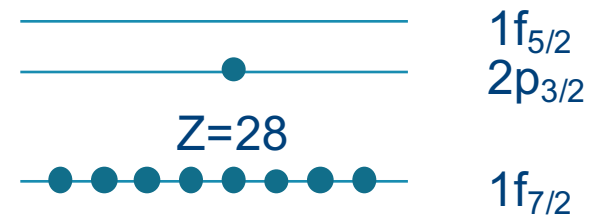
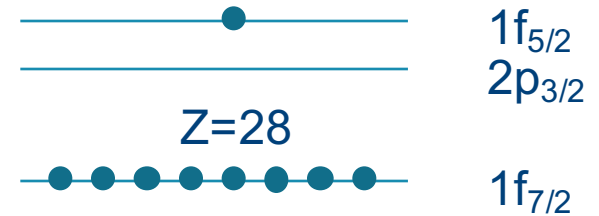
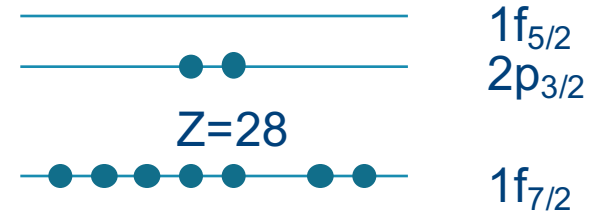
# Introduction



# Focus of the research



States in  $^{71}\text{Cu}$



Protons in  $^{71}\text{Cu}$

# Physics motivation

## Experimental observations

VOLUME 81, NUMBER 15

PHYSICAL REVIEW LETTERS

12 October 1998

### Beta Decay of $^{68-74}\text{Ni}$ and Level Structure of Neutron-Rich Cu Isotopes

S. Franchoo, M. Huyse, K. Kruglov, Y. Kudryavtsev, W. F. Mueller, R. Raabe, I. Reusen, P. Van Duppen, J. Van Roosbroeck, L. Vermeeren, and A. Wöhr\*

*Instituut voor Kern- en Stralingsfysica, University of Leuven, B-3001 Leuven, Belgium*

K.-L. Kratz and B. Pfeiffer

*Institut für Kernchemie, University of Mainz, D-55099 Mainz, Germany*

W. B. Walters

*Department of Chemistry, University of Maryland, College Park, Maryland 20742*

(Received 12 May 1998)

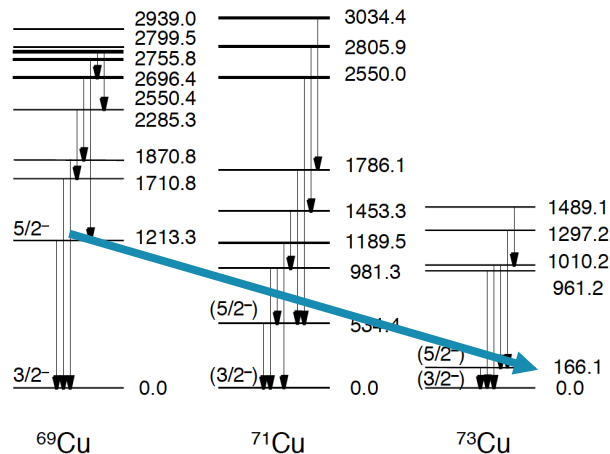


FIG. 4. Energy level systematics for  $^{69,71,73}\text{Cu}$ . Energies are given in keV. The data for  $^{69}\text{Cu}$  are taken from Ref. [18].

PRL 103, 142501 (2009)

PHYSICAL REVIEW LETTERS

week ending  
2 OCTOBER 2009

### Nuclear Spins and Magnetic Moments of $^{71,73,75}\text{Cu}$ : Inversion of $\pi 2p_{3/2}$ and $\pi 1f_{5/2}$ Levels in $^{75}\text{Cu}$

K. T. Flanagan,<sup>1,2</sup> P. Vingerhoets,<sup>1</sup> M. Avgoulea,<sup>1</sup> J. Billowes,<sup>3</sup> M. L. Bissell,<sup>1</sup> K. Blaum,<sup>4</sup> B. Cheal,<sup>3</sup> M. De Rydt,<sup>1</sup> V. N. Fedosseev,<sup>5</sup> D. H. Forest,<sup>6</sup> Ch. Geppert,<sup>7,8</sup> U. Köster,<sup>10</sup> M. Kowalska,<sup>11</sup> J. Krämer,<sup>9</sup> K. L. Kratz,<sup>9</sup> A. Krieger,<sup>9</sup> E. Mané,<sup>3</sup> B. A. Marsh,<sup>5</sup> T. Materna,<sup>10</sup> L. Mathieu,<sup>12</sup> P. L. Molkanov,<sup>13</sup> R. Neugart,<sup>9</sup> G. Neyens,<sup>1</sup> W. Nörtershäuser,<sup>9,7</sup> M. D. Seliverstov,<sup>13,16</sup> O. Serot,<sup>12</sup> M. Schug,<sup>4</sup> M. A. Sjoedin,<sup>17</sup> J. R. Stone,<sup>14,15</sup> N. J. Stone,<sup>14,15</sup> H. H. Stroke,<sup>18</sup> G. Tugate,<sup>6</sup> D. T. Yordanov,<sup>4</sup> and Yu. M. Volkov<sup>13</sup>

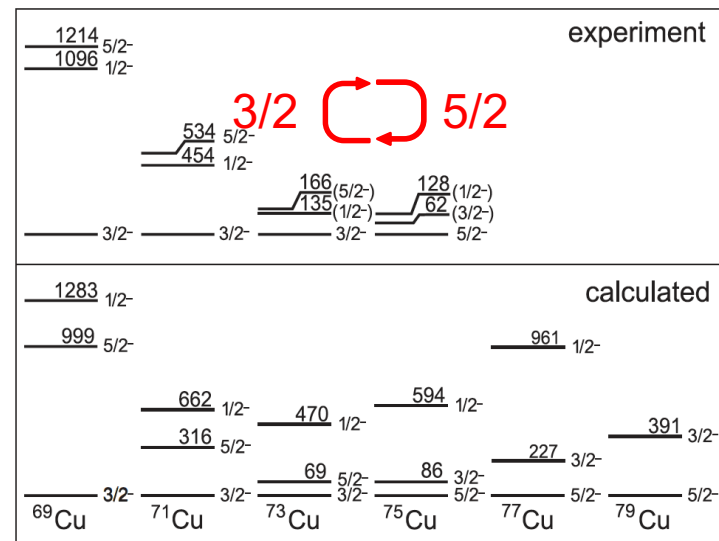
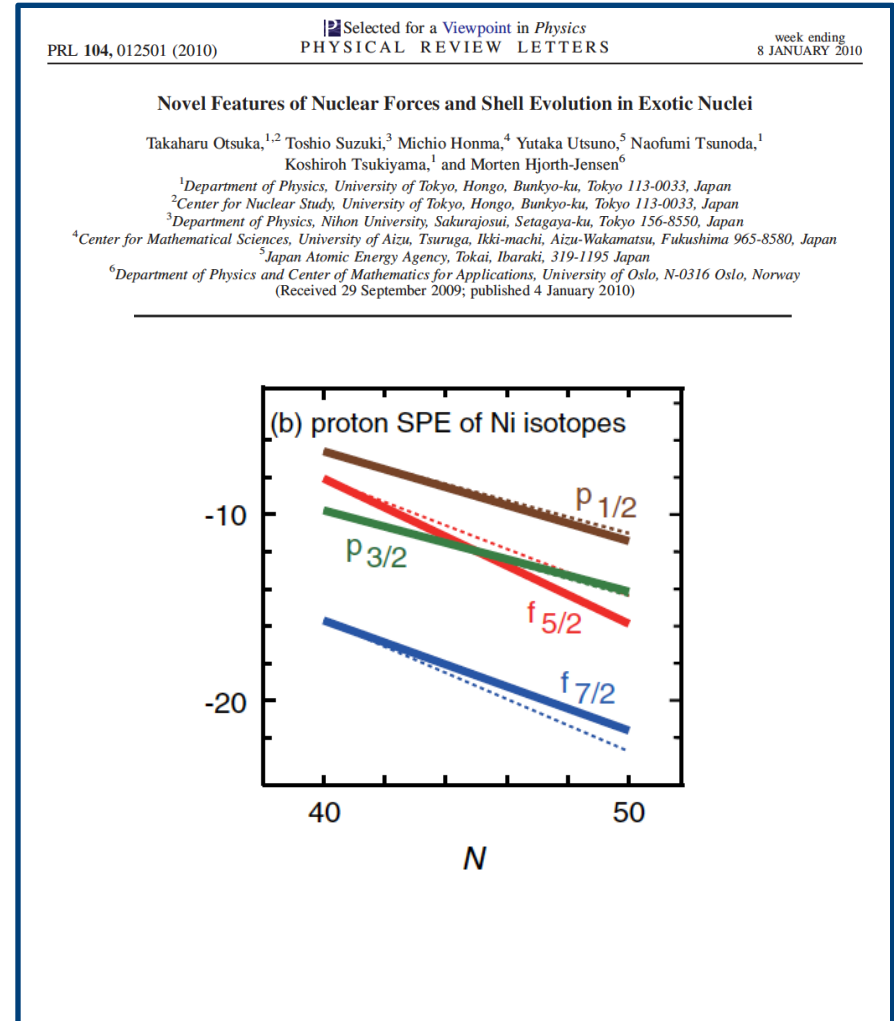
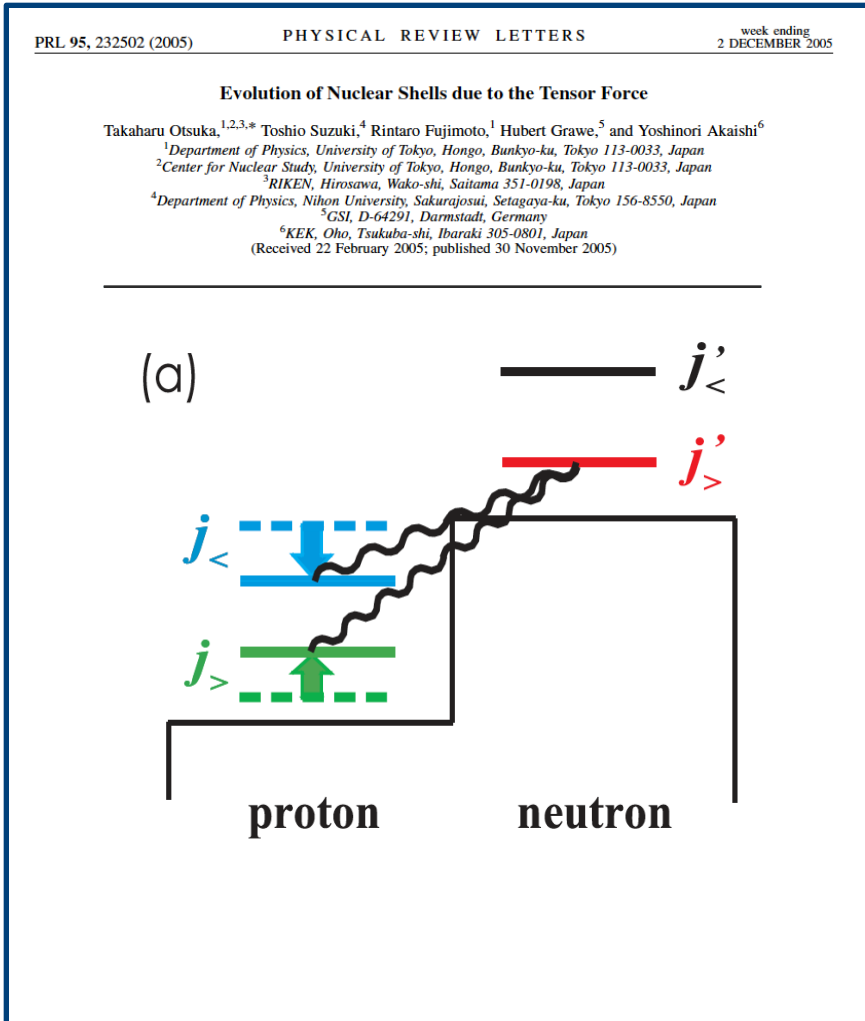


FIG. 3. Energy of the lowest levels from experiment [2,5,6] compared to large-scale shell-model calculation [25].

# Physics motivation

## Theoretical explanations

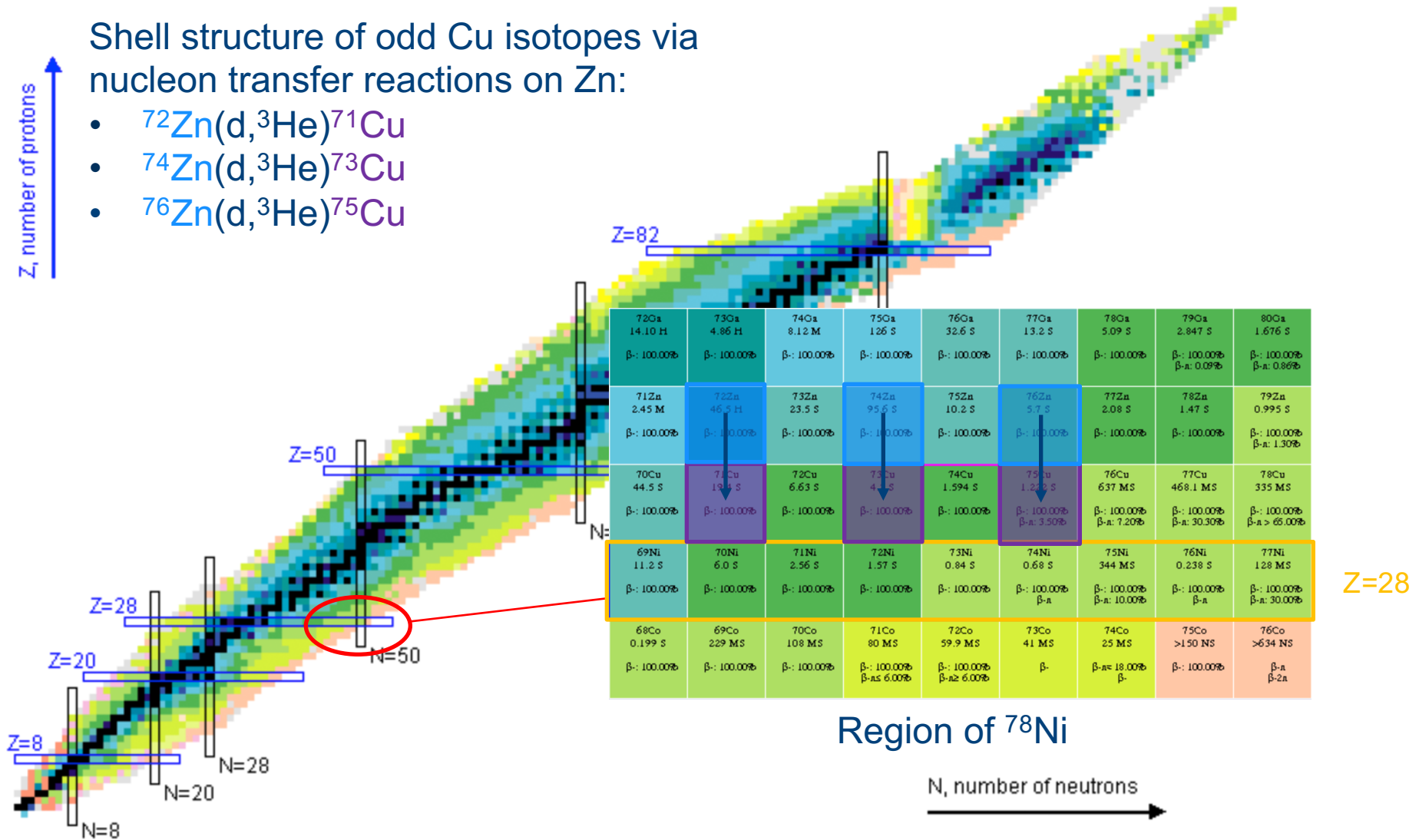


# Focus of the research

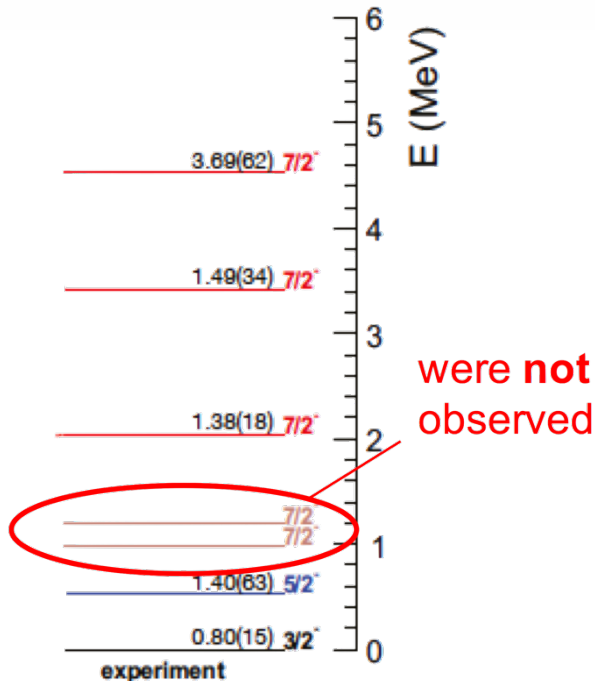
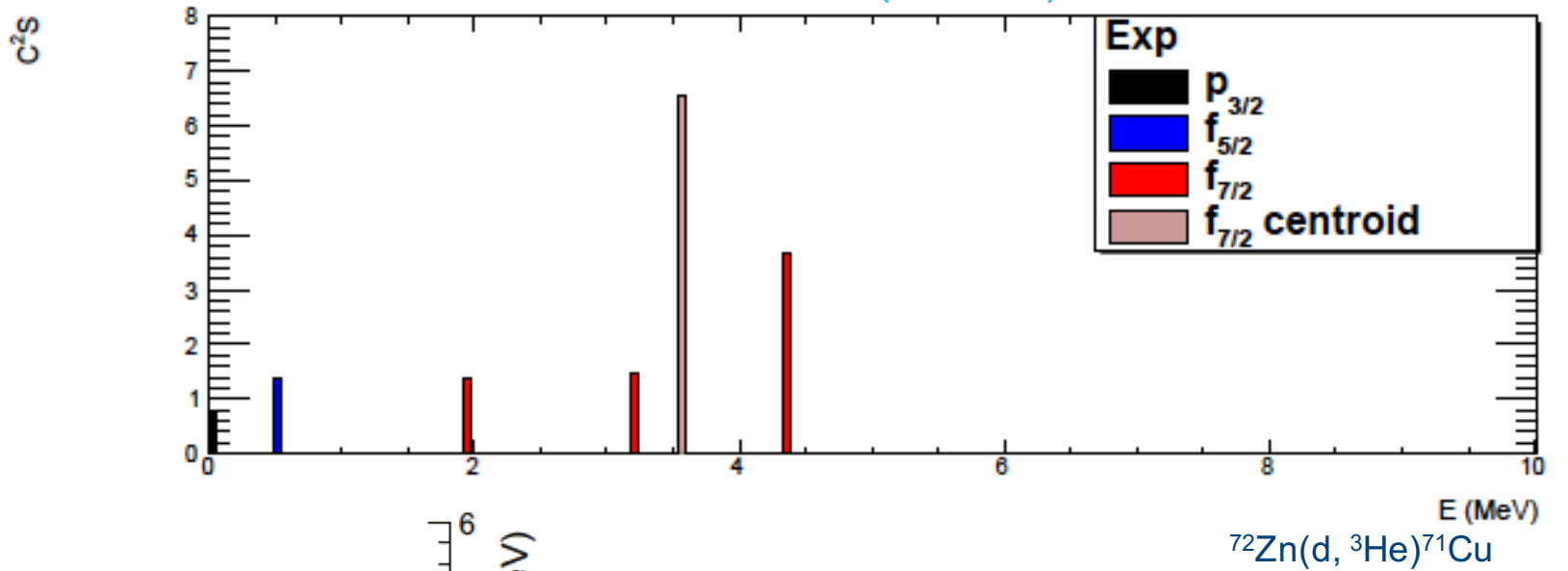
Shell structure of odd Cu isotopes via nucleon transfer reactions on Zn:

- $^{72}\text{Zn}(d, ^3\text{He})^{71}\text{Cu}$
- $^{74}\text{Zn}(d, ^3\text{He})^{73}\text{Cu}$
- $^{76}\text{Zn}(d, ^3\text{He})^{75}\text{Cu}$

Z, number of protons



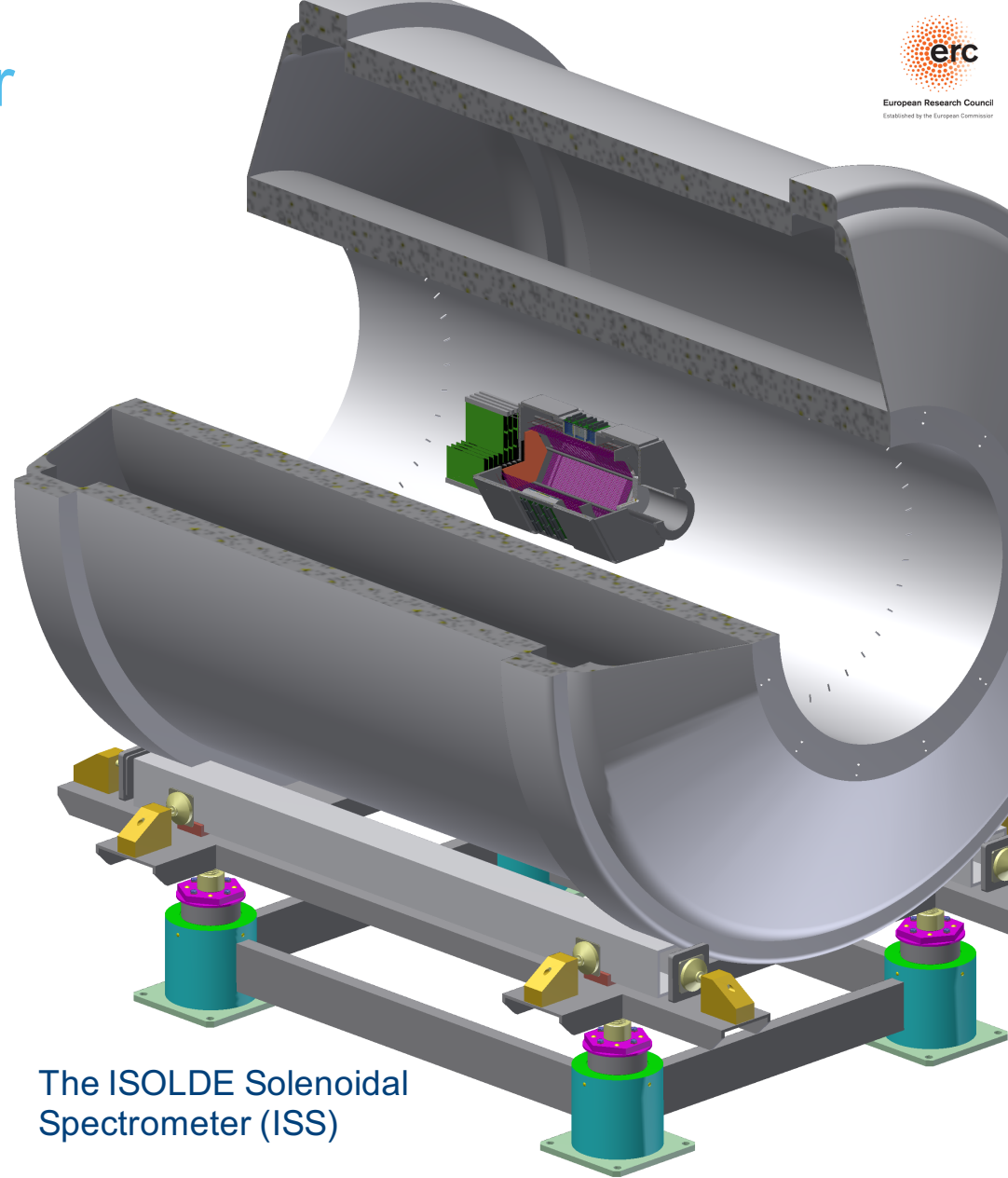
# What has been measured via (d,<sup>3</sup>He) on Zn?



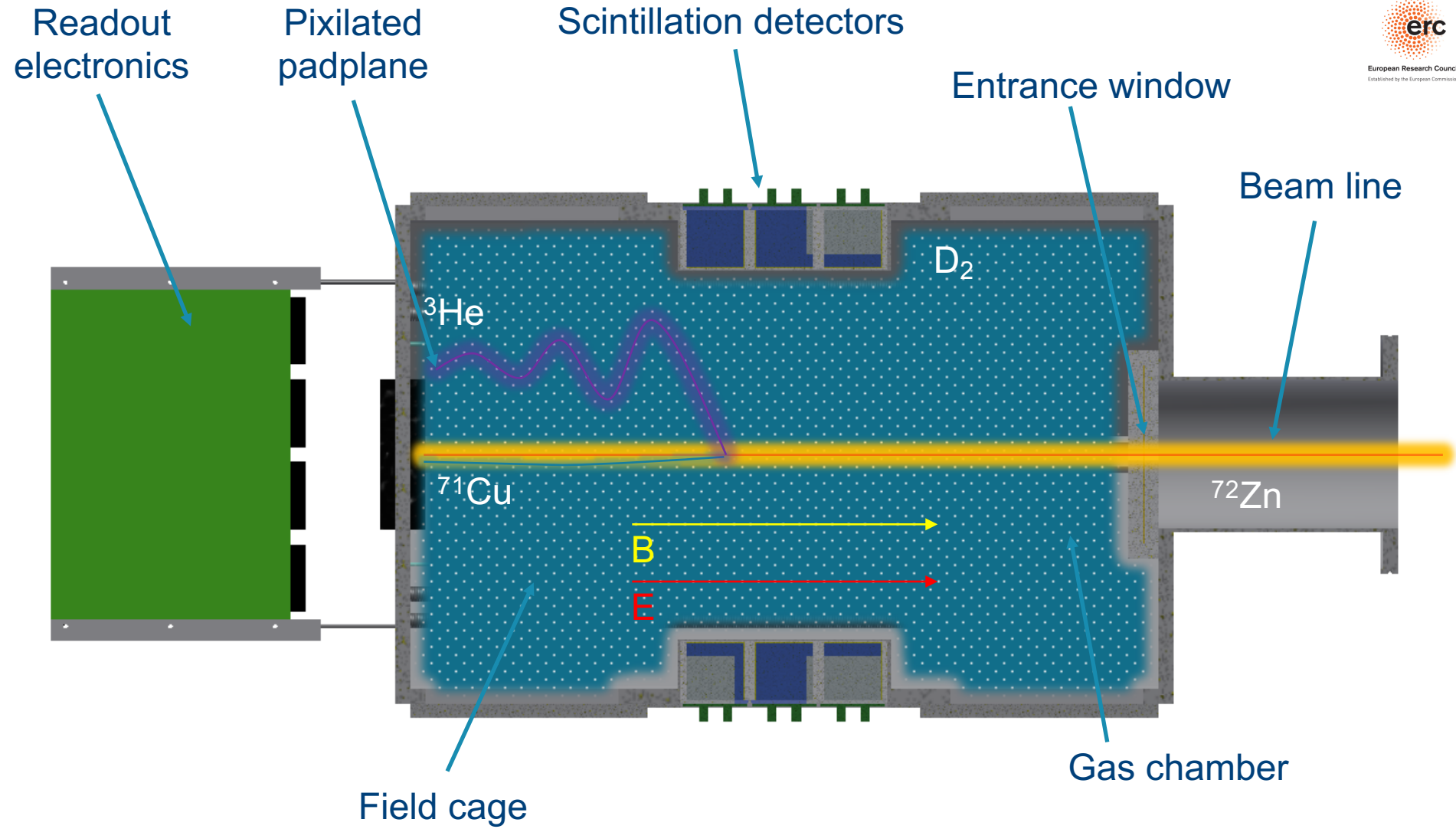
1. Possibility of studying orbital positions via (d,<sup>3</sup>He) in inverse kinematics
2. Transfer reactions selectively populate states with a strong single-particle character
3. (d,<sup>3</sup>He) is ideal for mapping Z=28 energy gap by scanning energy difference between  $f_{3/2}/f_{5/2}$  and  $f_{7/2}$  orbitals with rising number of neutrons

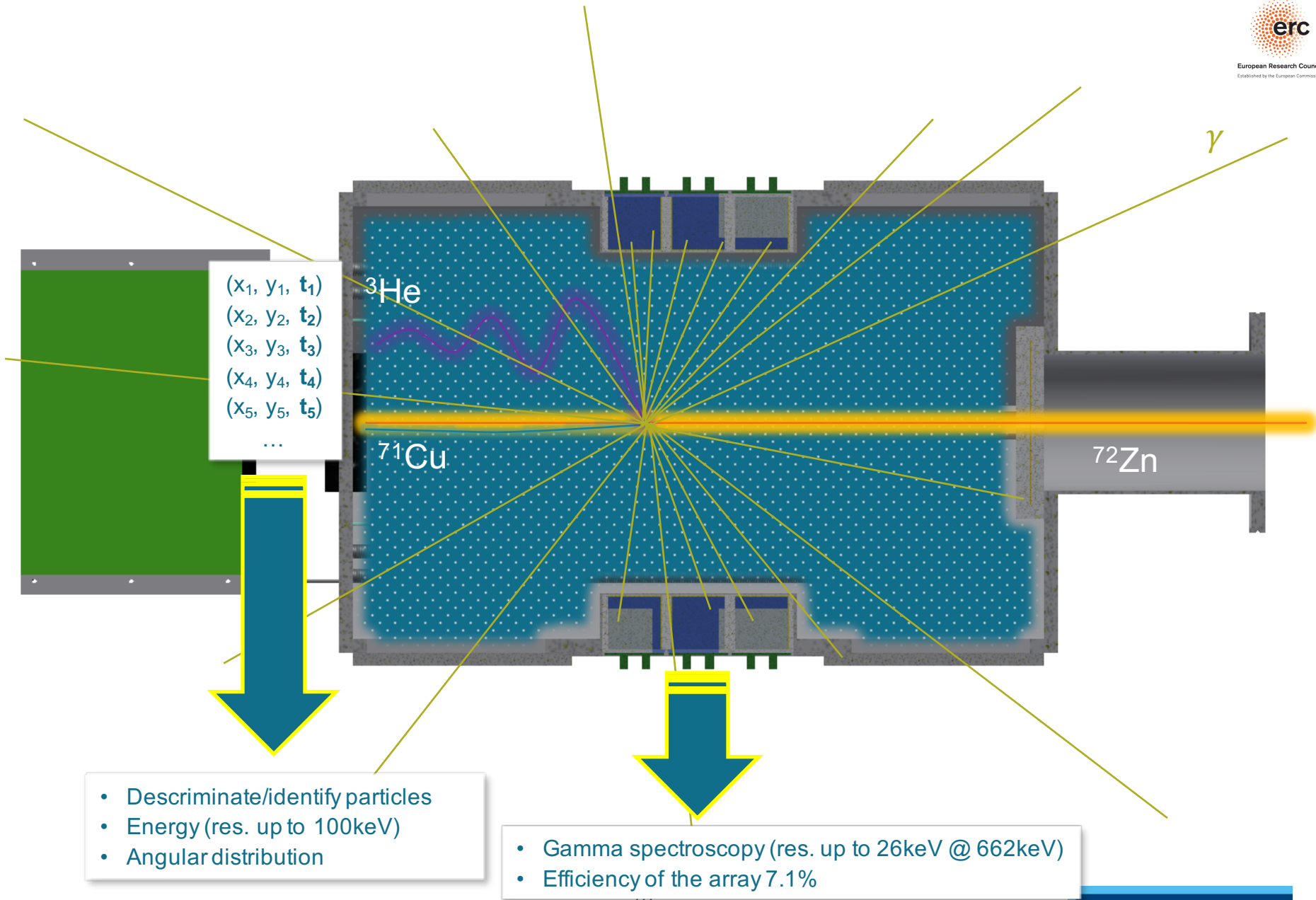
# The SpecMAT detector

- TPC will be surrounded by a gamma-ray detection array.
- Detector will be placed in a high magnetic field (up to 3T).



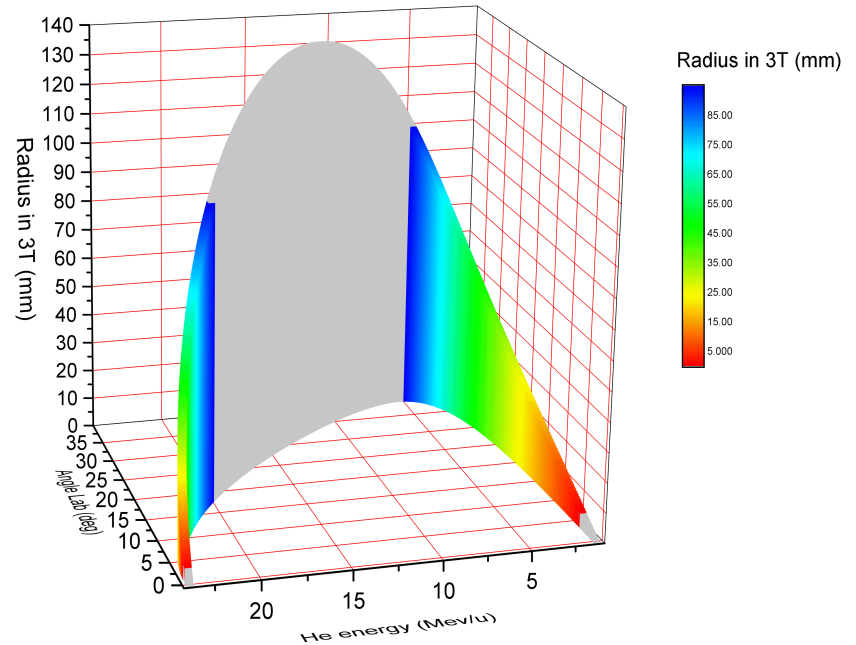
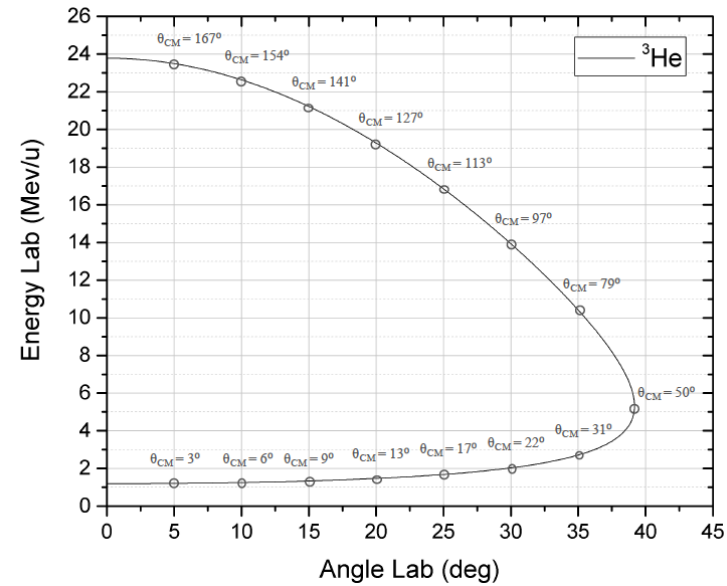
The ISOLDE Solenoidal Spectrometer (ISS)





# Kinematic plot

- To identify  $^3\text{He}$ , cyclotron radius of  $^3\text{He}$  has to be smaller than 100mm
- With the limit at 100mm radius,  $^3\text{He}$  could be detected with:
  - up to  $40^\circ$  in lab
  - up to  $50^\circ$  in CMS



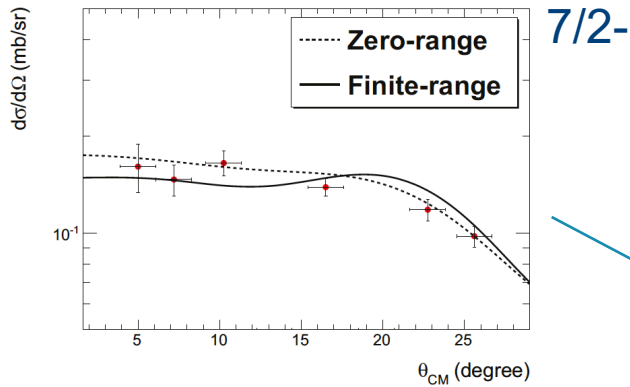


Figure 6.10: *Differential cross-section compared to the DWBA calculation for the state at 3.35 MeV*

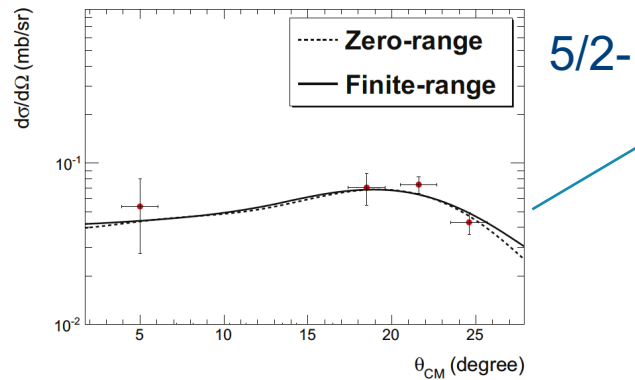
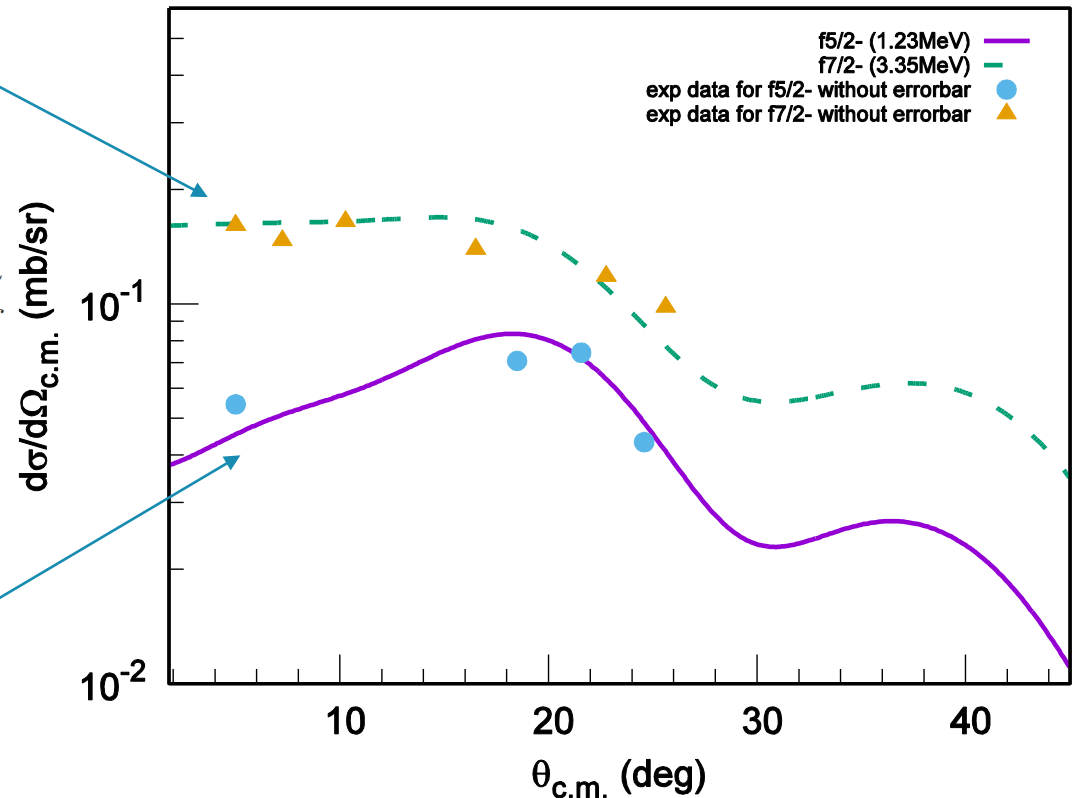


Figure 6.7: *Differential cross-section compared to the DWBA calculation for the state at 1.23 MeV*



With high luminosity of the SpecMAT detector we expect to complete angular distribution up to  $45 - 50^\circ$  in CMS

# Beam request

Run	Beam	Energy [MeV/u]	Yield [ions/ $\mu\text{C}$ ]	Estimated beam intensity at SpecMAT [pps]	Estimated gamma+ $^3\text{He}$ detection rate [events/shift]	Requested shifts			Total
						Beam tuning	Laser ON	Laser OFF	
1 <sup>st</sup>	<b><math>^{72}\text{Zn}</math></b>	10	$7 \cdot 10^7$	$5 \cdot 10^6$	113.6	2	9	2	<b>13</b>
2 <sup>nd</sup>	<b><math>^{74}\text{Zn}</math></b>	10	$6.9 \cdot 10^7$	$4.92 \cdot 10^6$	111.7	2	9	2	<b>13</b>
	<b><math>^{76}\text{Zn}</math></b>	10	$1.7 \cdot 10^7$	$1.14 \cdot 10^6$	25.9	2	20	3	<b>25</b>

# TAC remarks

- **Large number of shifts:** we would like to divide 51 shifts into two runs 13 shifts and 38 shifts, estimated 2 or 3 UC<sub>x</sub> targets depending on the target stability
- **RILIS optics is unstable:** under investigation by RILIS group; less critical than for very exotic isotopes
- We would like to know energy resolution and beam profile
- **Allowed energy spread and beam size:** even 5% of beam energy uncertainty might give only up to 50 keV of uncertainty to <sup>3</sup>He energy, beam size up to  $\varnothing$  10mm
- Above remarks do not have significant effect on the feasibility of experiment
- These experiments are preferable @ 10MeV/u

# Thank you for your attention!

O. Poleshchuk<sup>1</sup>, R. Raabe<sup>1</sup>, H. Alvarez-Pol<sup>2</sup>, M. Babo<sup>1</sup>, B. Bastin<sup>3</sup>, B. Blank<sup>4</sup>, M. Caamaño<sup>2</sup>,  
S. Ceruti<sup>1</sup>, F. de Oliveira Santos<sup>2</sup>, N. de Sereville<sup>5</sup>, B. Duclos<sup>3</sup>, H. De Witte<sup>1</sup>,  
B. Fernandez-Dominguez<sup>2</sup>, F. Flavigny<sup>5</sup>, S. Franchoo<sup>5</sup>, L. Gaffney<sup>6</sup>, J. Giovinazzo<sup>4</sup>, T. Goigoux<sup>4</sup>, G.F. Grinyer<sup>3</sup>,  
F. Hammache<sup>5</sup>, A. Illana<sup>1</sup>, A.T. Laffoley<sup>3</sup>, T. Marchi<sup>1</sup>, B. Mauss<sup>3</sup>, J. Pancin<sup>3</sup>, J.L. Pedroza<sup>4</sup>, J. Pibernat<sup>4</sup>, E.C. Pollacco<sup>7</sup>,  
F. Renzi<sup>1</sup>, T. Roger<sup>3</sup>, F. Saillant<sup>3</sup>, P. Sizun<sup>7</sup>, D. Suzuki<sup>8</sup>,  
J.A. Swartz<sup>9</sup>, G. Wittwer<sup>3</sup>, J. Yang<sup>1,10</sup>

<sup>1</sup>*KU Leuven, Instituut voor Kern- en Stralingsfysica, Celestijnenlaan 200D, 3001 Leuven, Belgium*

<sup>2</sup>*Universidade de Santiago de Compostela, 15706 Santiago de Compostela, Spain*

<sup>3</sup>*Grand Accélérateur National d'Ions Lourds (GANIL), CEA/DRF-CNRS/IN2P3, Bvd Henri Becquerel, 14076 Caen, France*

<sup>4</sup>*Centre d'Études Nucléaires de Bordeaux Gradignan, Université Bordeaux 1, CNRS/IN2P3, Chemin de Solarium, 33175 Gradignan, France*

<sup>5</sup>*Institut de Physique Nucléaire Orsay, CNRS/IN2P3, Université Paris-Sud, Université Paris-Saclay, 91406 Orsay, France*

<sup>6</sup>*SOLDE, CERN, CH-1211 Geneva 23, Switzerland*

<sup>7</sup>*CEA, Centre de Saclay, IRFU/SPhN 91191 Gif-sur-Yvette, France*

<sup>8</sup>*RIKEN Nishina Center, 2-1 Hirosawa, Wako, Saitama 351-0198, Japan*

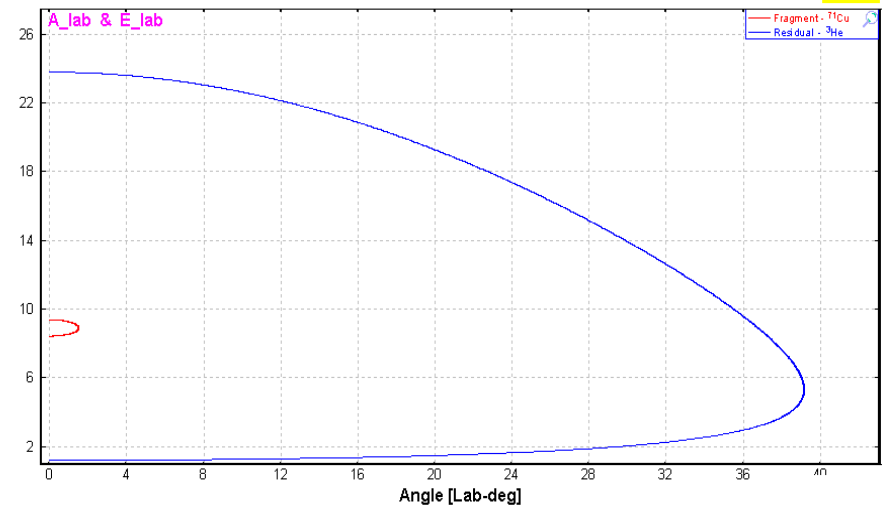
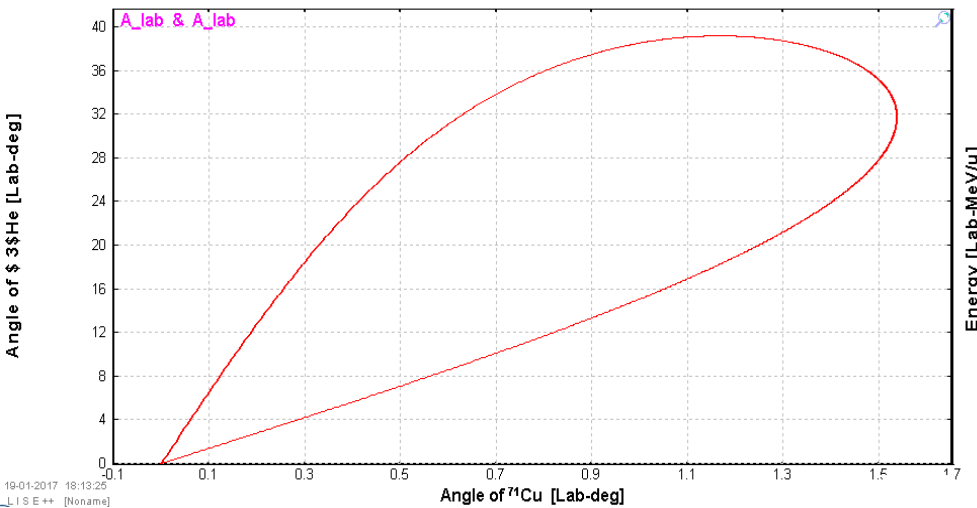
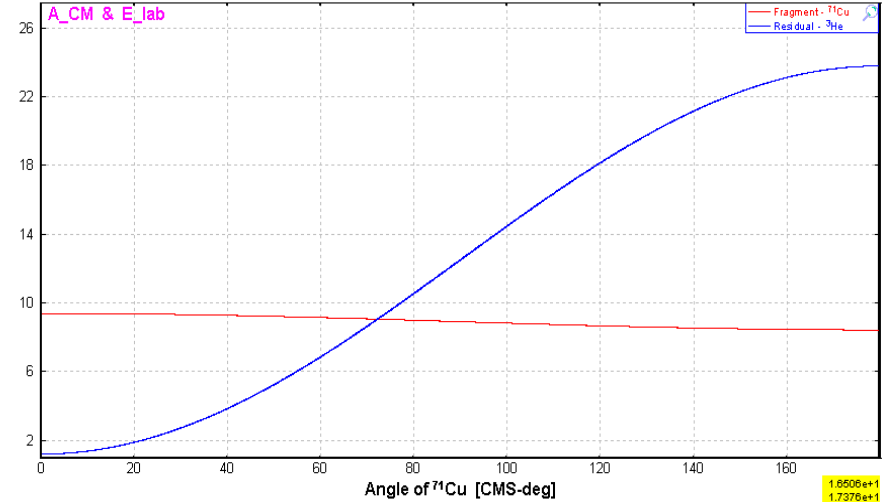
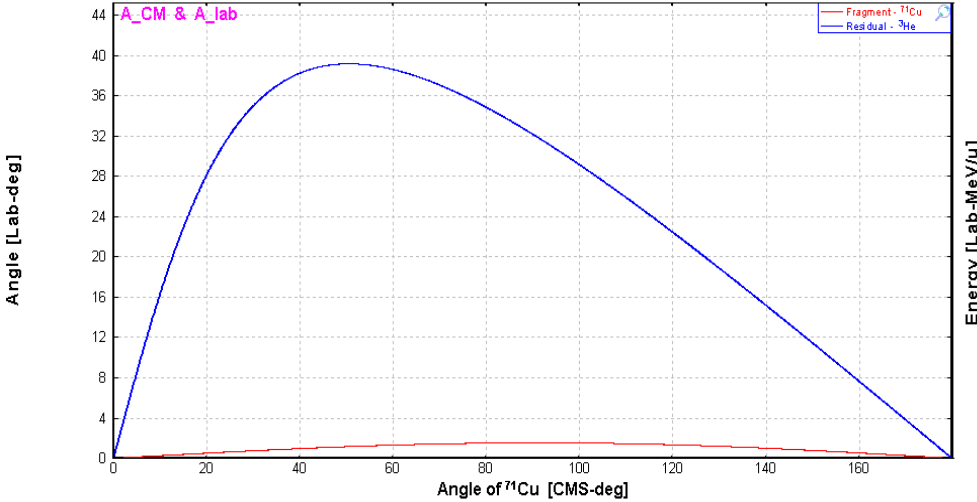
<sup>9</sup>*Aarhus University, Department of Physics and Astronomy, DK-8000 Aarhus C, Denmark*

<sup>10</sup>*Physique Nucleaire Théorique, Université Libre de Bruxelles, B-1050 Bruxelles, Belgium*

# Backup slides

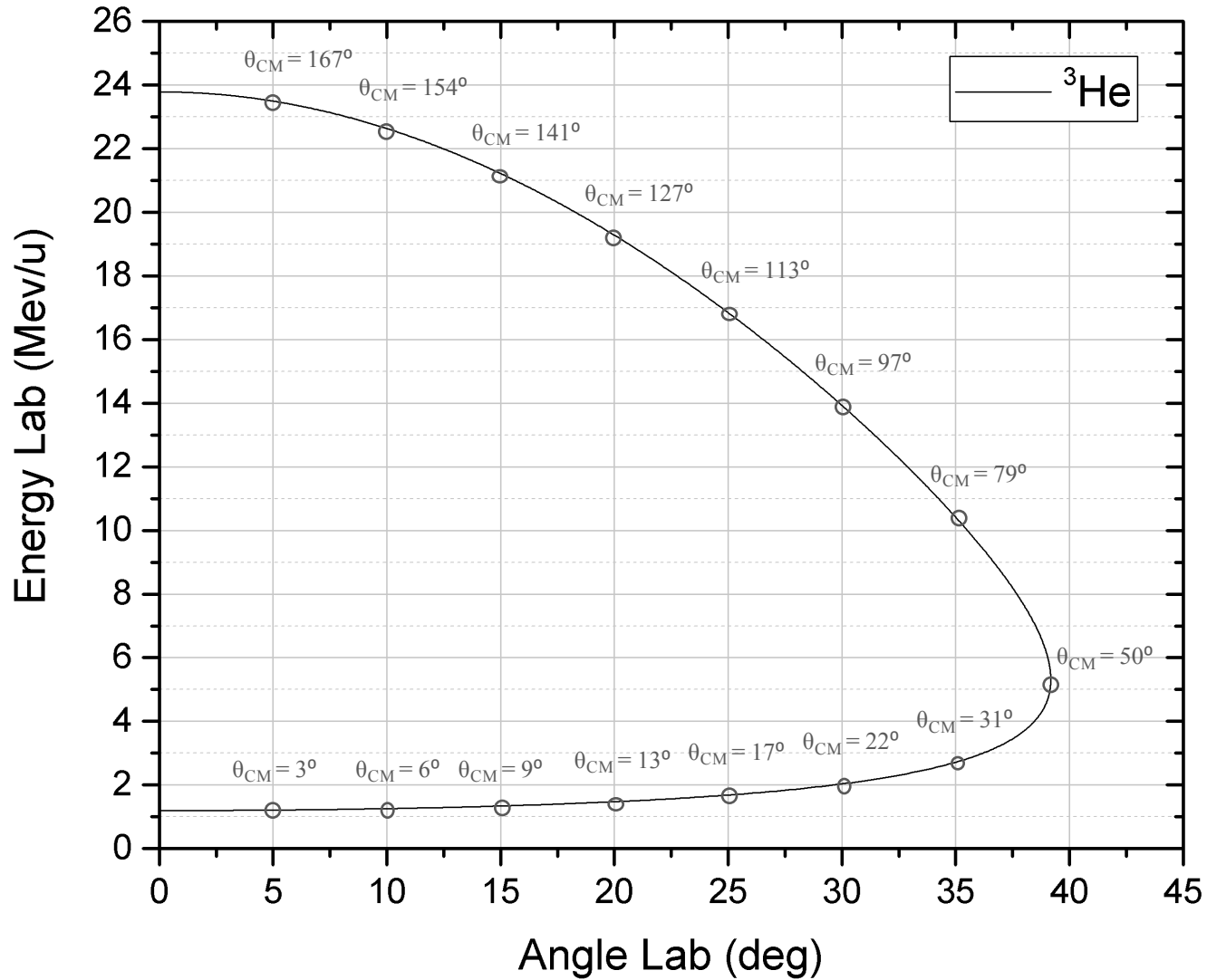
# Kinematics plots

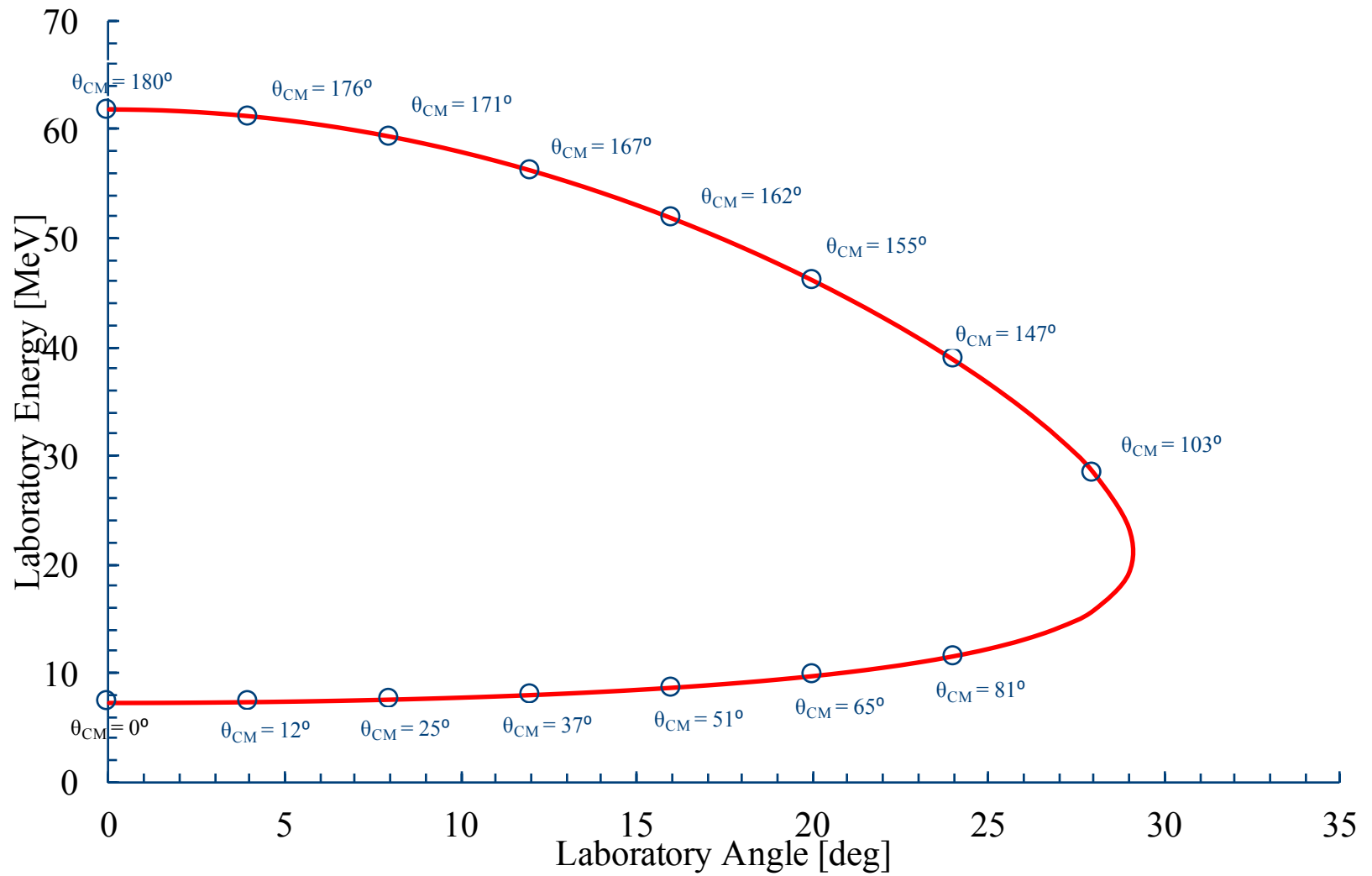
$^{72}\text{Zn} + ^2\text{H} \Rightarrow ^{71}\text{Cu} + ^3\text{He}$   $^2\text{H}(^{72}\text{Zn}, ^{71}\text{Cu})^3\text{He}$ ; Reaction at the "middle" of the target  
 Projectile Energy at the reaction place: 9.40 MeV/u    Grazing angle: CMS = 17.21 deg; Lab = 0.44 deg  
 Q reaction : -7.23 MeV (Excitations 0.0+0.0=>0.0+0.0); Plotted Energy option is "after reaction"



19-01-2017 18:13:25  
L1SE++ [None]

# Kinematic plot





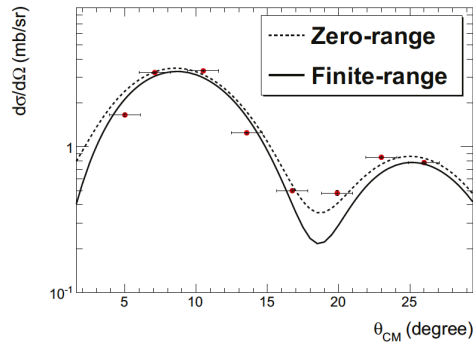


Figure 6.5: *Differential cross-section compared to the DWBA calculation for the ground state*

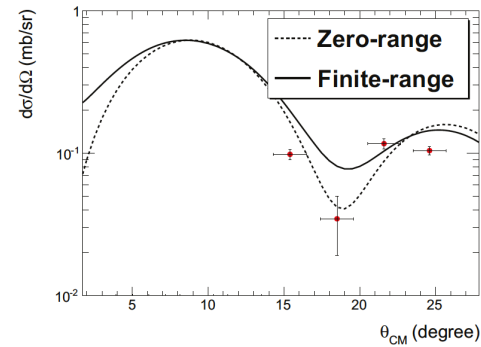


Figure 6.6: *Differential cross-section compared to the DWBA calculation for the state at 1.11 MeV*

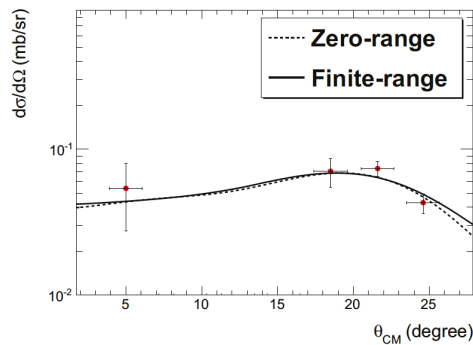


Figure 6.7: *Differential cross-section compared to the DWBA calculation for the state at 1.23 MeV*

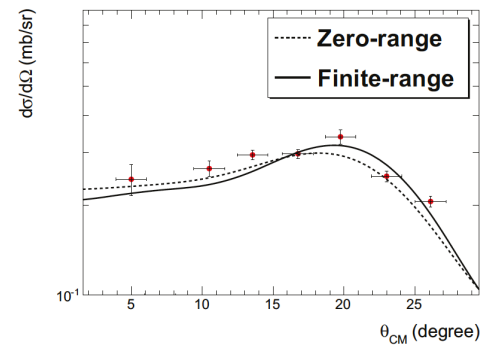


Figure 6.8: *Differential cross-section compared to the DWBA calculation for the state at 1.71 MeV*

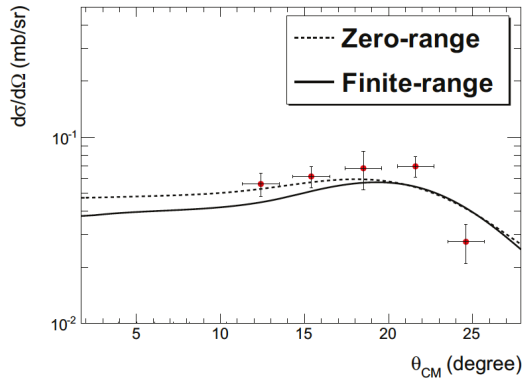


Figure 6.9: *Differential cross-section compared to the DWBA calculation for the state at 1.87 MeV*

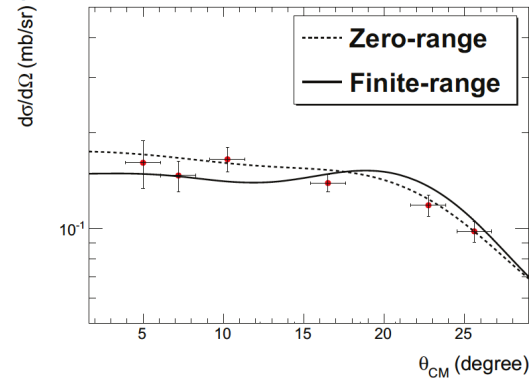


Figure 6.10: *Differential cross-section compared to the DWBA calculation for the state at 3.35 MeV*

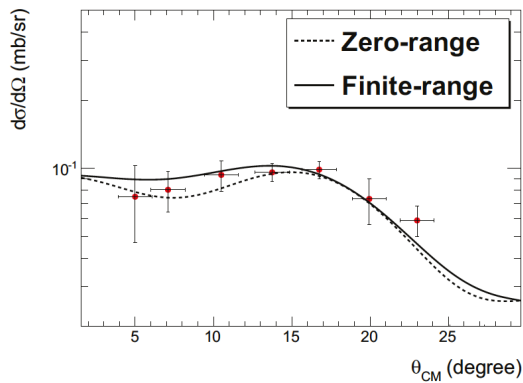


Figure 6.11: *Differential cross-section compared to the DWBA calculation for the state at 3.70 MeV*

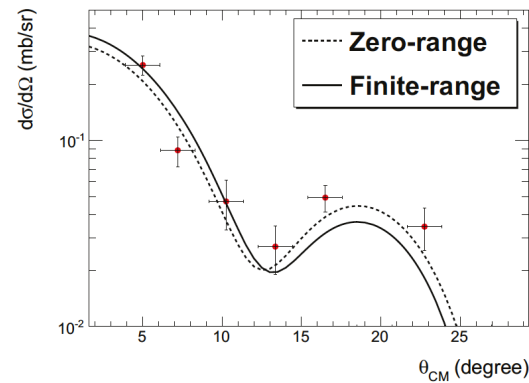
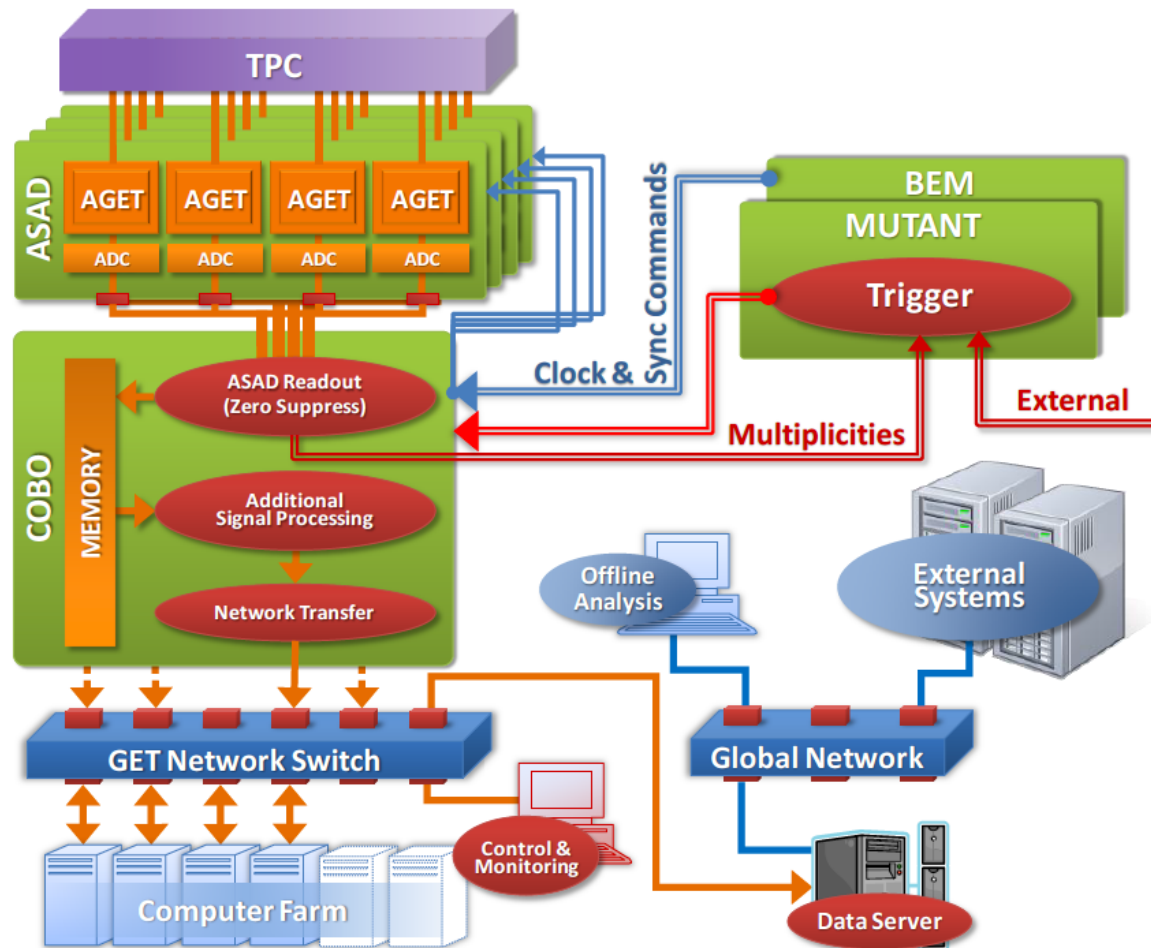


Figure 6.12: *Differential cross-section compared to the DWBA calculation for the state at 3.94 MeV*

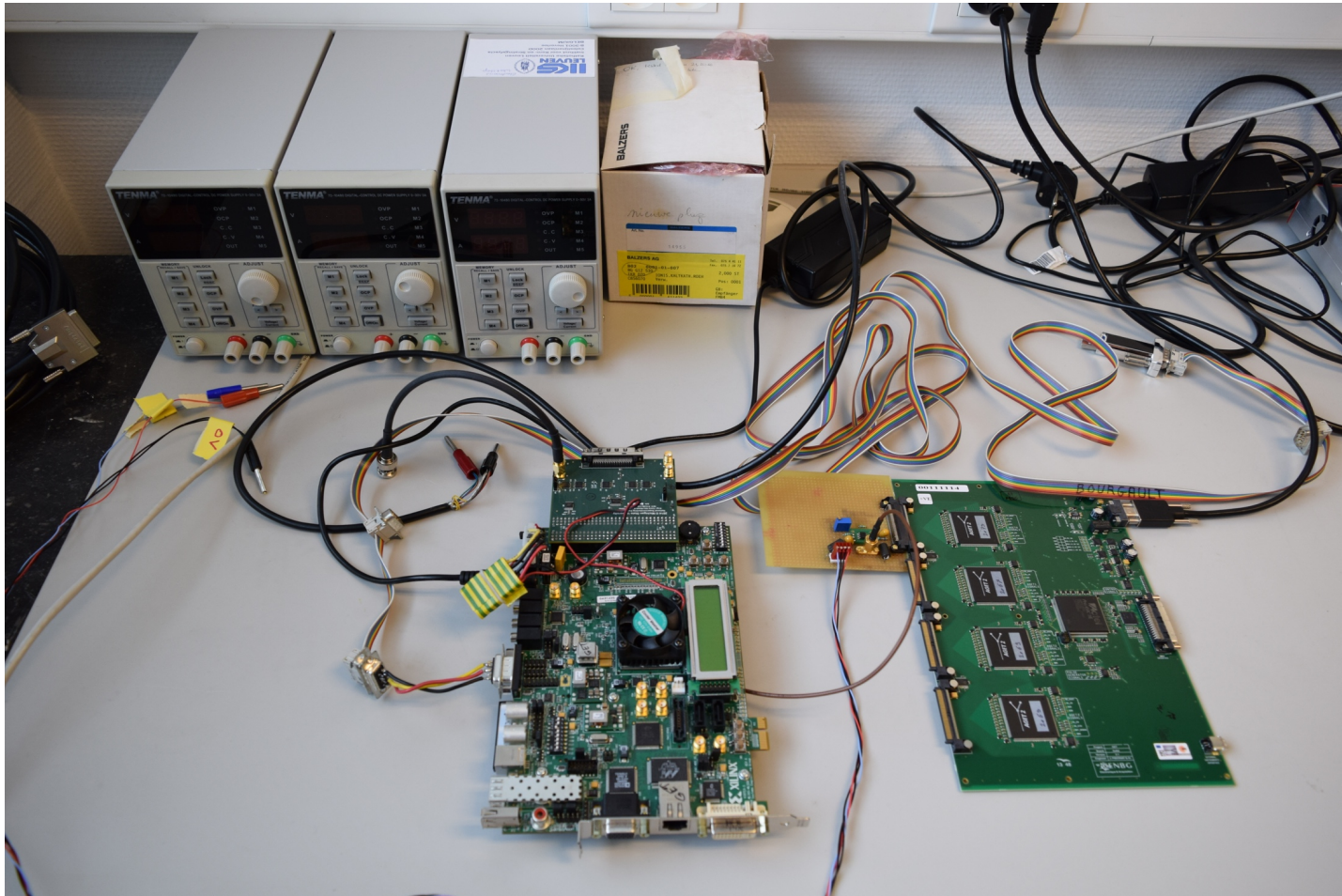
Total cross sections for population low lying states in  $^{69}\text{Cu}$  via  $(\text{d}, ^3\text{He})$  reaction based on the experiment of Morfouace et. al.

Isotope	State	Energy [MeV]	Estimated total cross-section [mb]
$^{69}\text{Cu}$	g.s. $3/2^-$	0	0.82
	$5/2^-$	1.23	0.04
	$7/2^-$	1.71	0.19
	$7/2^-$	1.87	0.03
	$7/2^-$	3.35	0.11
	$7/2^-$	3.7	0.05
	$7/2^-$	3.94	0.03

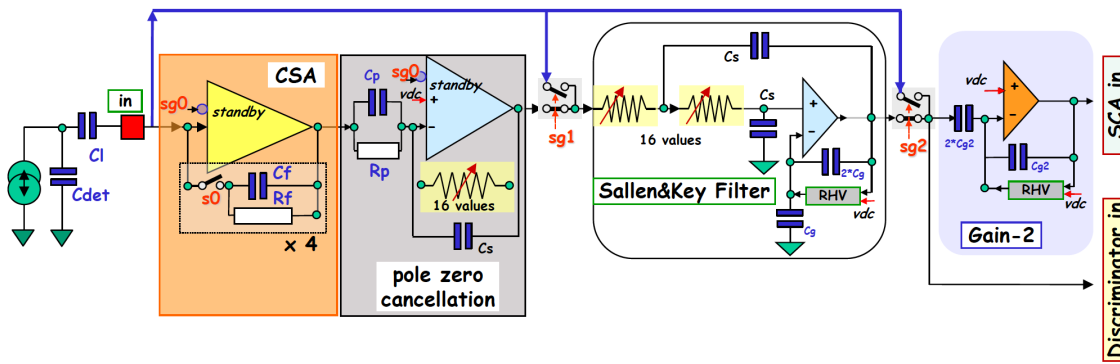
# GET electronics for TPC



Overview of GET



**R-CoBo (Reduced Concentration Board) and AsAd (ASIC Support & Analog-Digital conversion)**



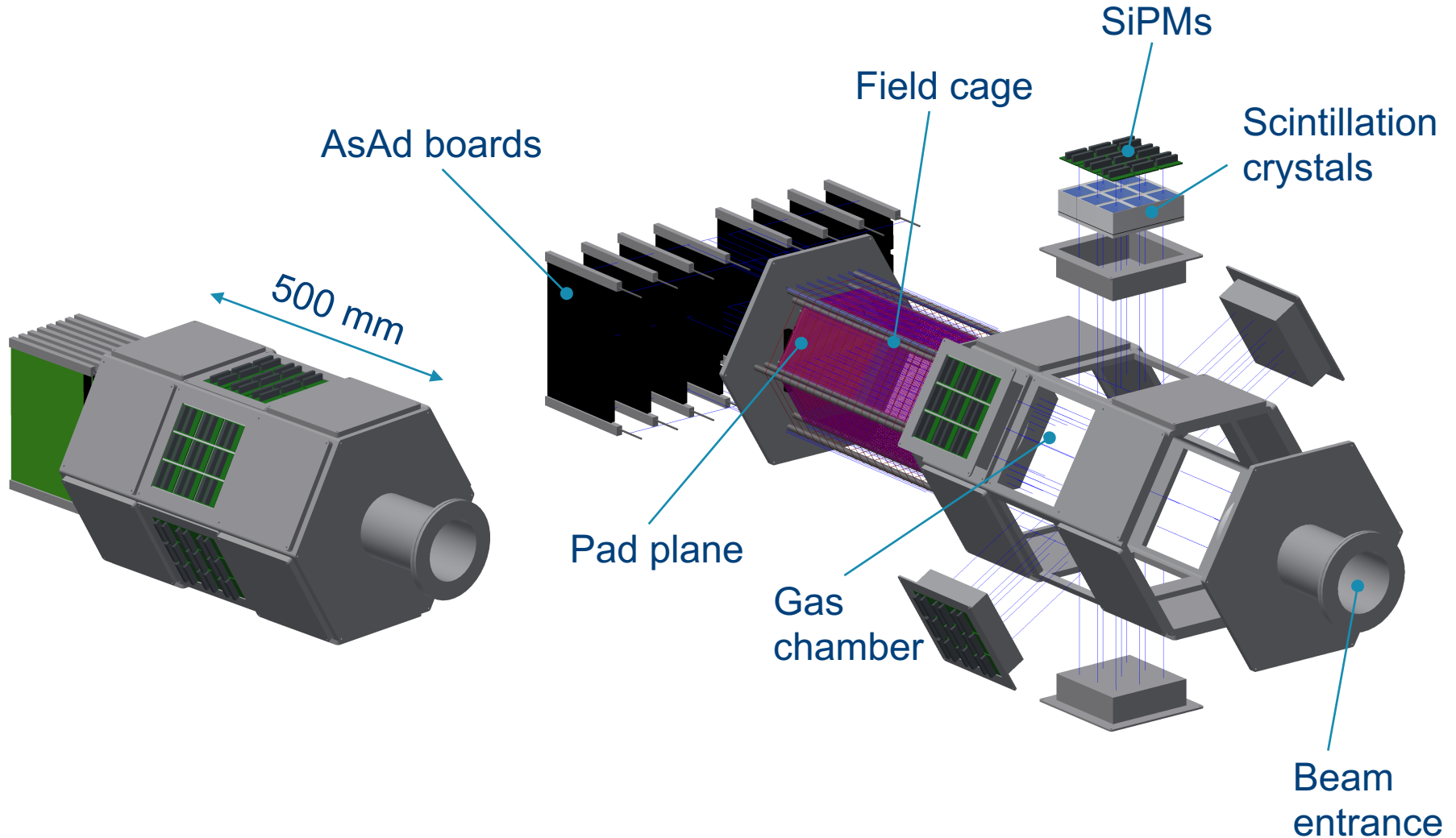
Parameter	Value
Polarity of detector signal	Negative or Positive
Number of channels	72
External Preamplifier	Yes; access to the filter or SCA input
<b>Charge measurement</b>	
Input dynamic range	120 fC; 1 pC; 10 pC
Gain	Adjustable/(channel)
Output dynamic range	2V p-p
I.N.L	< 2%
Resolution	< 850 e <sup>-</sup> (Charge range: 120fC; Peaking Time: 200ns; Cinchannel. < 30pF)
<b>Sampling</b>	
Peaking time value	50 ns to 1 μs (16 values)
Number of SCA Time bins	511
Sampling Frequency	1 MHz to 100 MHz
<b>Time resolution</b>	
Jitter	60 ps rms
Skew	< 700 ps rms
<b>Trigger</b>	
Discriminator solution	L.E.D
Trigger Output/Multiplicity	OR of the 72 hit channel registers; Width = 2xTSCAckread
Dynamic range	5% of input charge range
I.N.L	< 5%
Threshold value	4-bit DAC/channel + (3-bit + polarity bit) common DAC
Minimum threshold value	≥ noise
<b>Readout</b>	
Readout frequency	20 MHz to 25 MHz
Channel Readout mode	Hit channel; specific channels; all channels
SCA Readout mode	511 cells; 256 cells; 128 cells
<b>Test</b>	
calibration	1 channel / 72; external test capacitor
test	1 channel / 72; internal test capacitor (1/charge range)
functional	1, few or 76 channels; internal test capacitor/channel
Counting rate	< 1 kHz
Power consumption	< 10 mW / channel

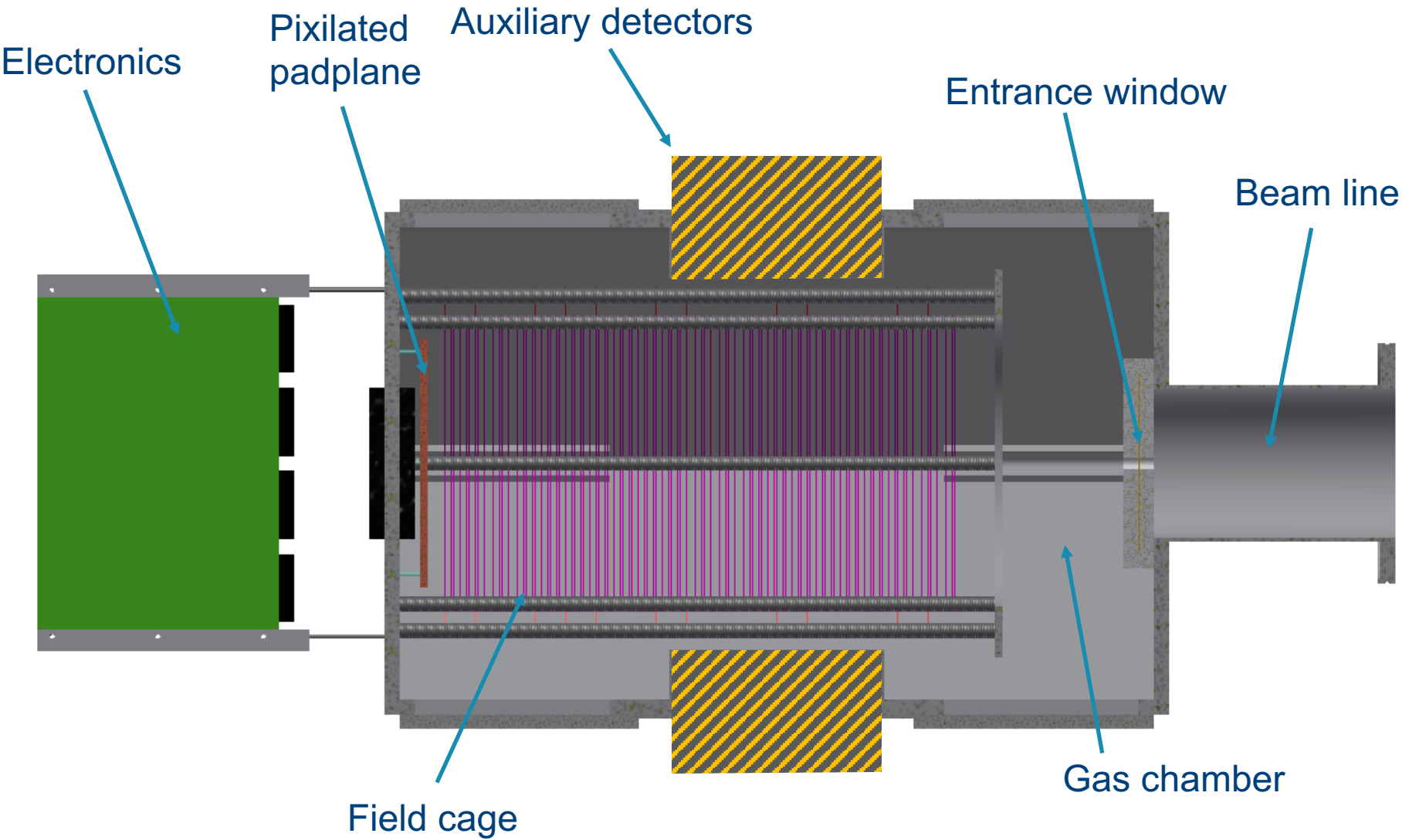
Table 1: The synthesis of the AGET requirements.



	AGET	CAEN 5780
Resolution	12 bit	14 bit
Sampling	100MHz	100MHz

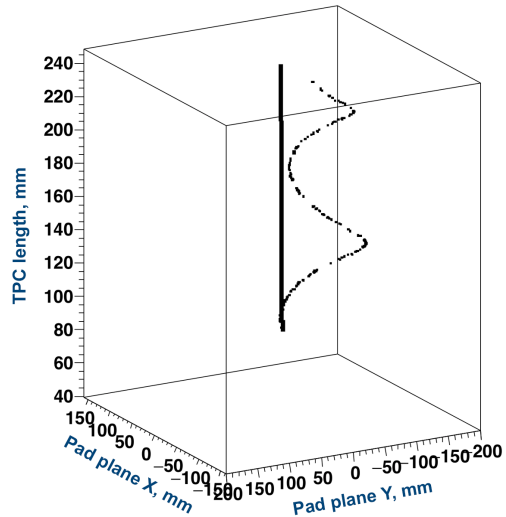
# Preliminary design of the SpecMAT detector



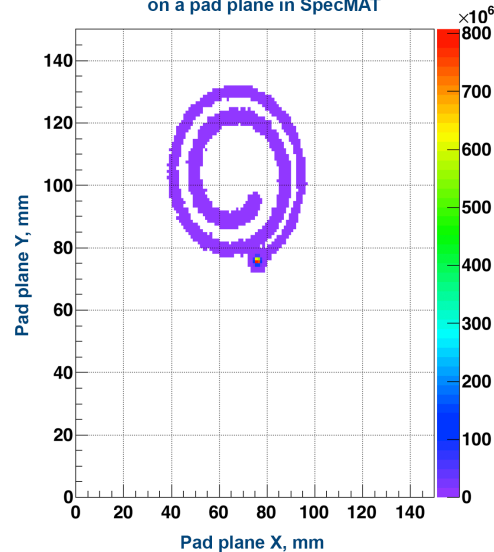


# Simulation of transfer reactions in GEANT4

Simulated tracks of reaction products,  
(proton and  $^{79}\text{Ni}$ ) in SpecMAT



Projection of a recoil proton trajectory  
on a pad plane in SpecMAT



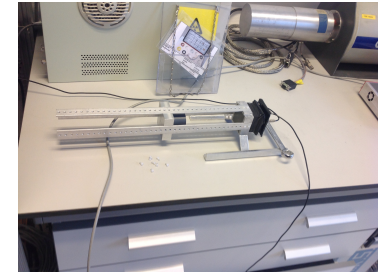
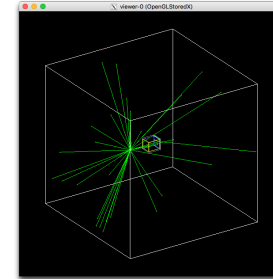
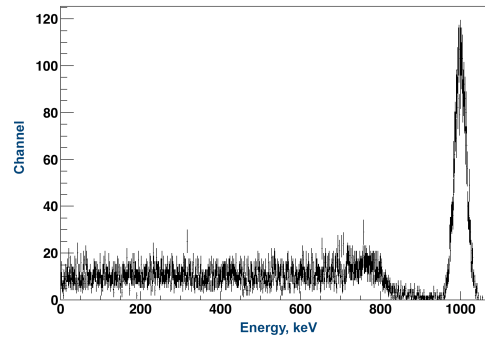
Simulation of  $^{78}\text{Ni}(d,p)^{79}\text{Ni}$  nuclear transfer reaction in inverse kinematics.

- $^{78}\text{Ni}$  @ 7,6 MeV/u.
- $\text{D}_2$  gas @ 1 atm.
- 4T magnetic field.

At HIE-ISOLDE, with post-accelerated ion beams at 10 MeV/u, transfer-reaction measurements will be possible also for negative Q-values and heavier nuclei.

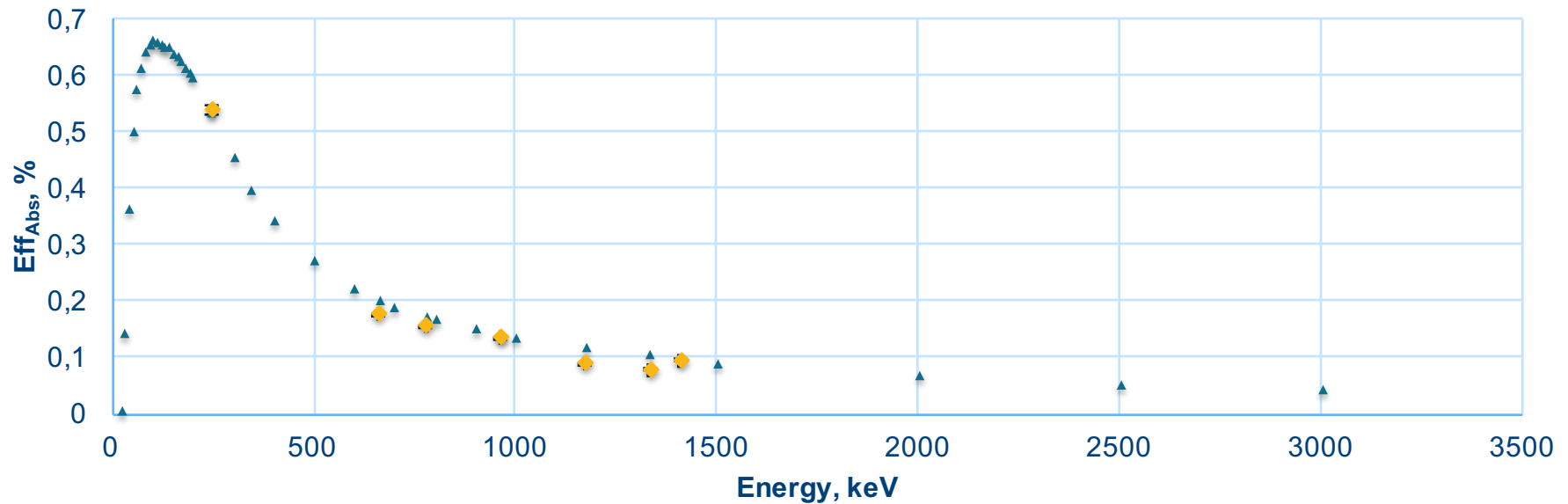
by T. Marchi

# Simulations of scintillator array in GEANT4

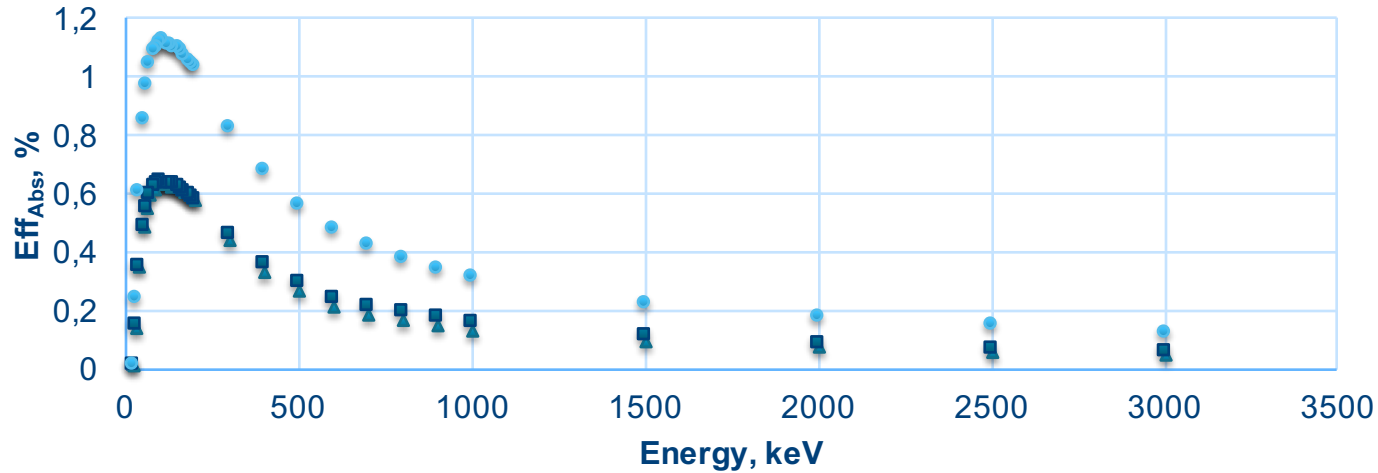


Our simulation is in a good agreement with experimentally measured  $\text{Eff}_{\text{Abs}}$  of 1,5''x1,5''x1,5''  $\text{CeBr}_3$  crystal, 120 mm away from sources

▲ Sim ◆ Exp

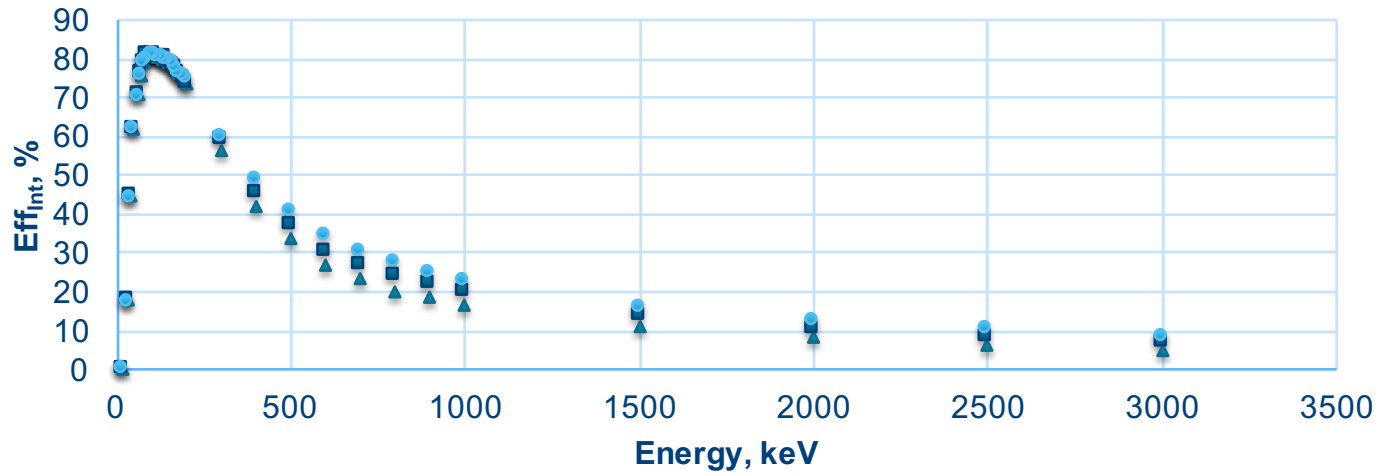


## Comparison of $\text{Eff}_{\text{Abs}}$

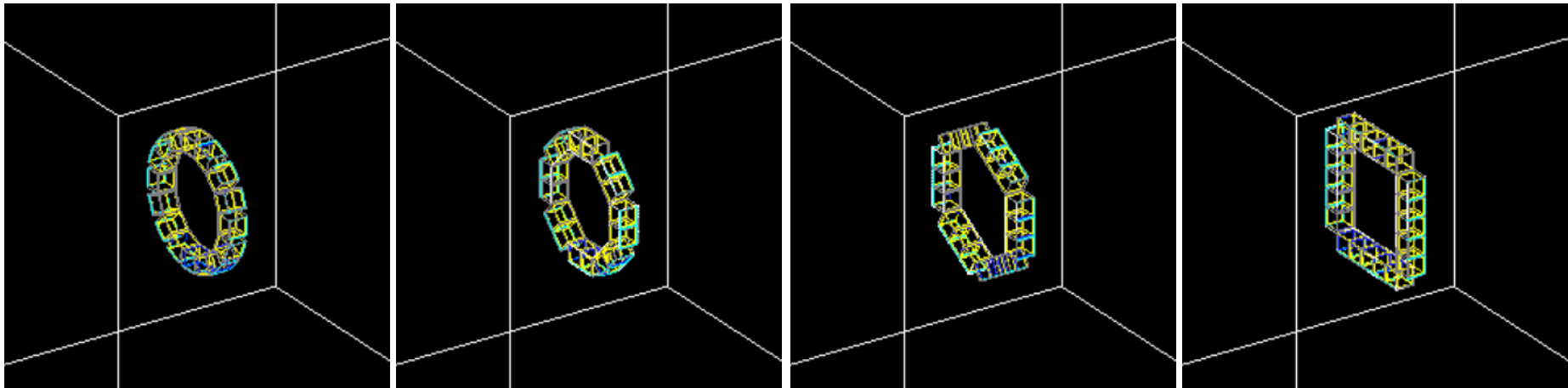


- ▲ 1,5"x1,5"x1,5", d=120mm
- 1,5"x1,5"x2", d=120mm
- 2"x2"x2", d=120mm

## Comparison of $\text{Eff}_{\text{Int}}$

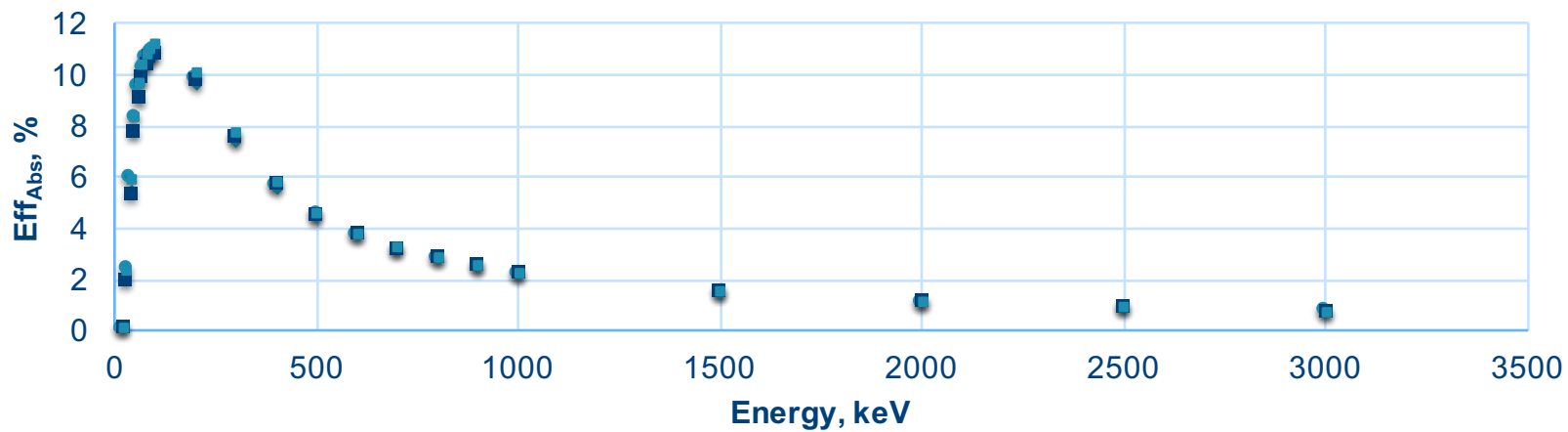


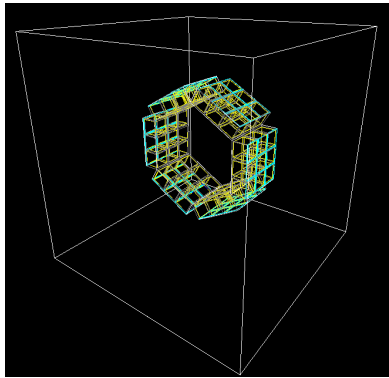
- ▲ 1,5"x1,5"x1,5", d=120mm
- 1,5"x1,5"x2", d=120mm
- 2"x2"x2", d=120mm



## Comparison of $\text{Eff}_{\text{Abs}}$ for different array shapes of 1,5"x1,5"x1,5" $\text{CeBr}_3$ crystals

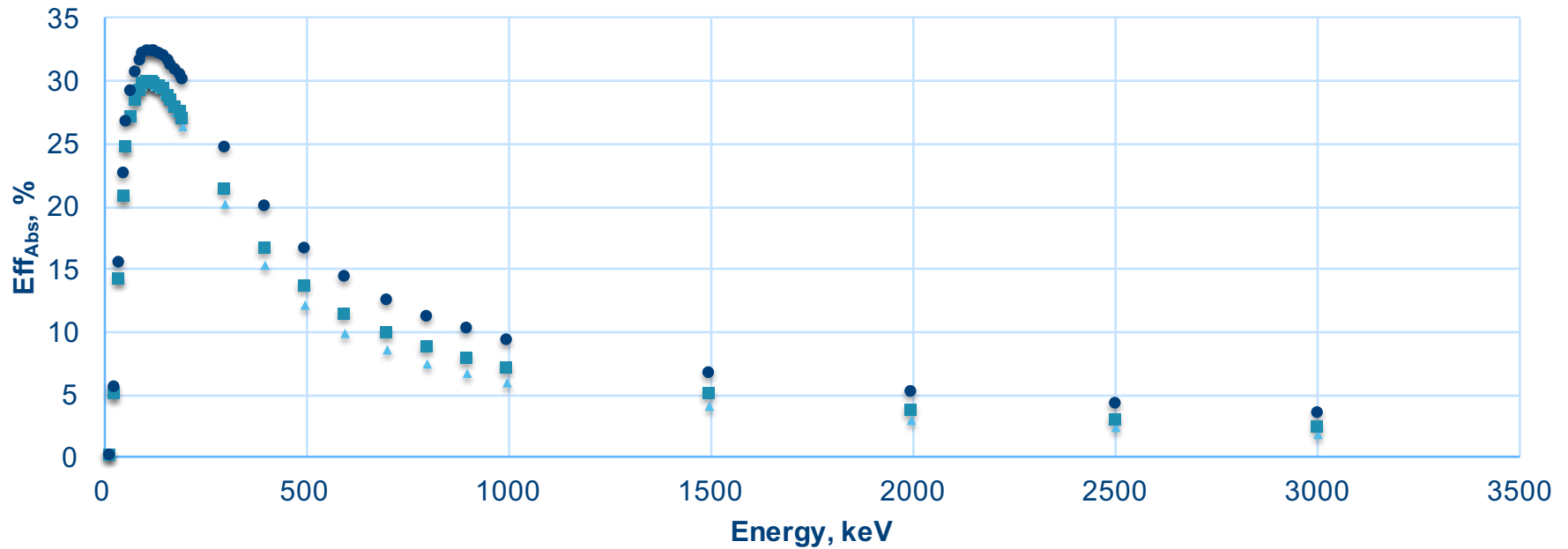
- Ring, 16cryst,  $R_{\text{in}}=115,629\text{mm}$  • Hex, 18cryst,  $R_{\text{in}}=119,512\text{mm}$
- Square, 20cryst,  $R_{\text{in}}=115\text{mm}$  ■ Octa, 16cryst,  $R_{in}=111,054\text{mm}$



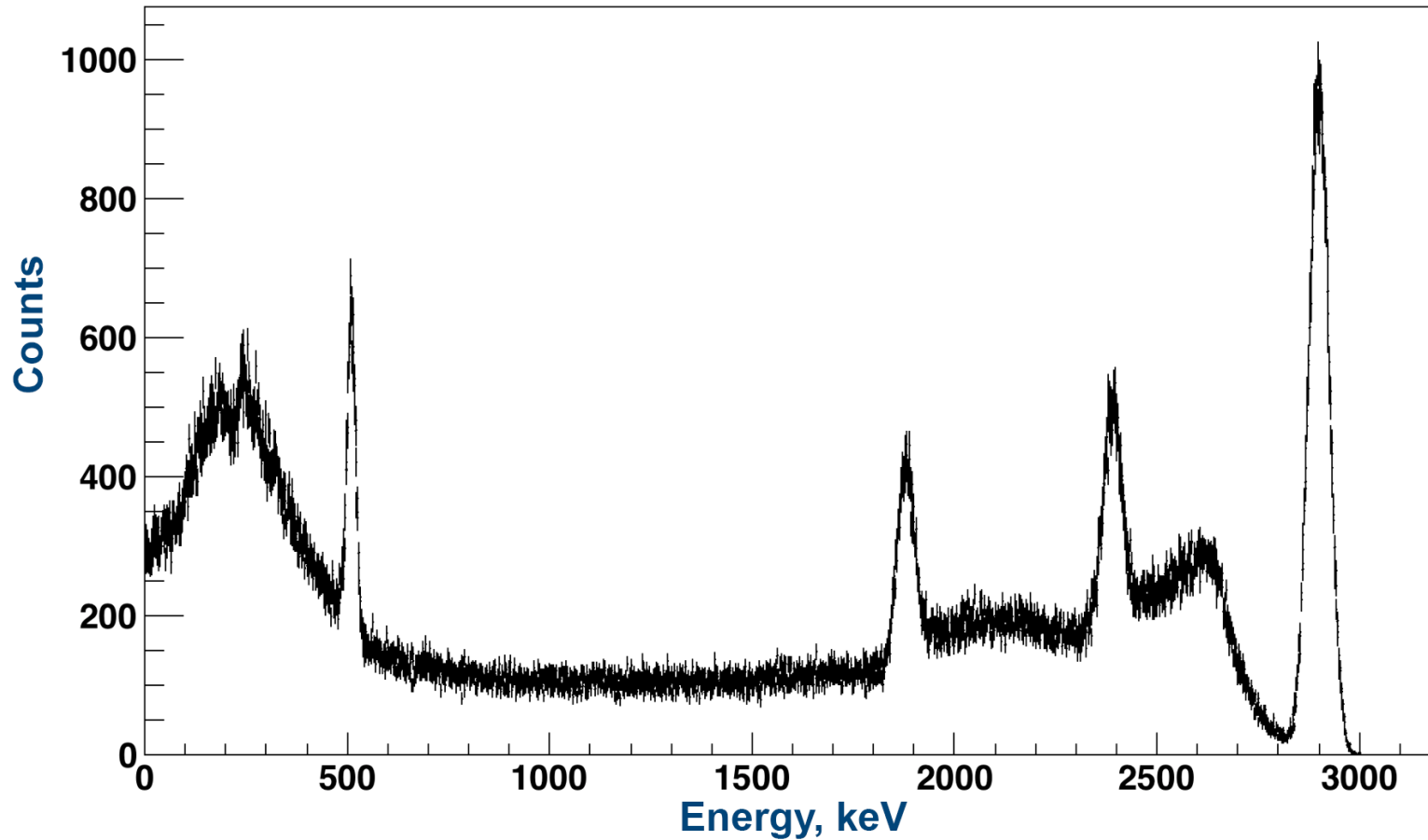


## Comparison of $\text{Eff}_{\text{Abs}}$ for 3 sizes of $\text{CeBr}_3$ crystals

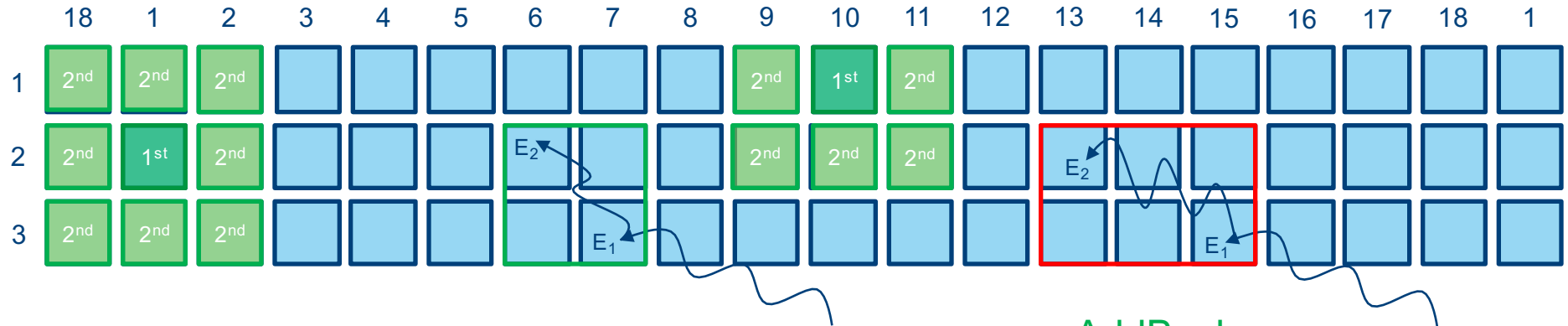
- ▲ Hex, 54cryst, 1,5"x1,5"x1,5",  $R_{\text{in}}=119,512\text{mm}$
- Hex, 54cryst, 1,5"x1,5"x2",  $R_{\text{in}}=119,512\text{mm}$
- Hex, 54cryst, 2"x2"x2",  $R_{\text{in}}=153,286\text{mm}$



## Energy spectrum obtained from simulation of detector array of 54 1,5''x1,5''x1,5'' CeBr<sub>3</sub> crystals arranged in hexagonal shape



# AddBack algorithm



Peak efficiency improvement via **increasing peak-to-total** ratio

Reconstruction of initial gamma energy from **scattered** or **escaped** gamma rays

AddBack

~~$E_1 = 422 \text{ keV}$~~

~~$E_2 = 240 \text{ keV}$~~

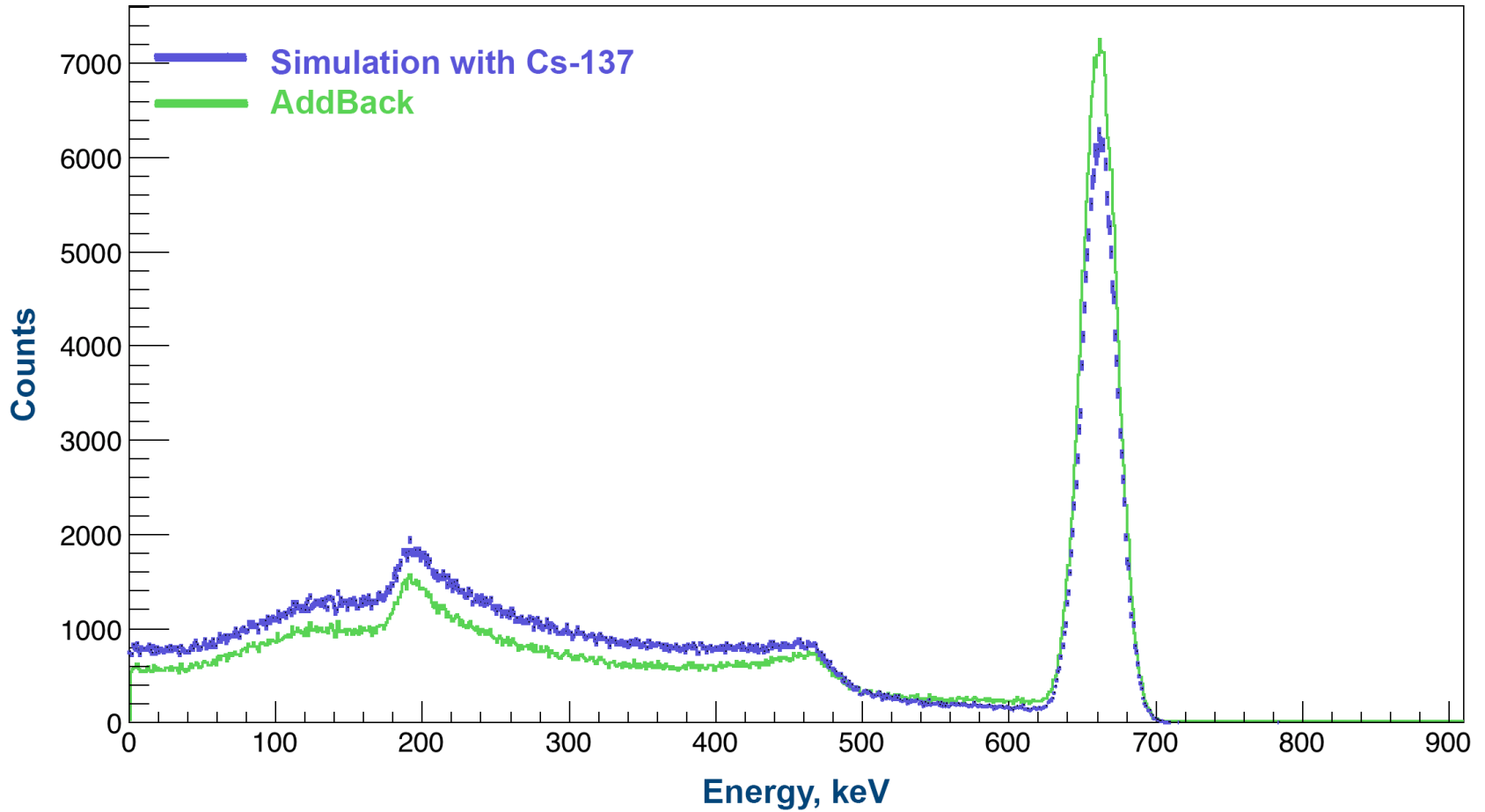
$$E_{\text{AddBack}} = E_1 + E_2 = 662 \text{ keV}$$

No AddBack

$$E_1 = 422 \text{ keV}$$

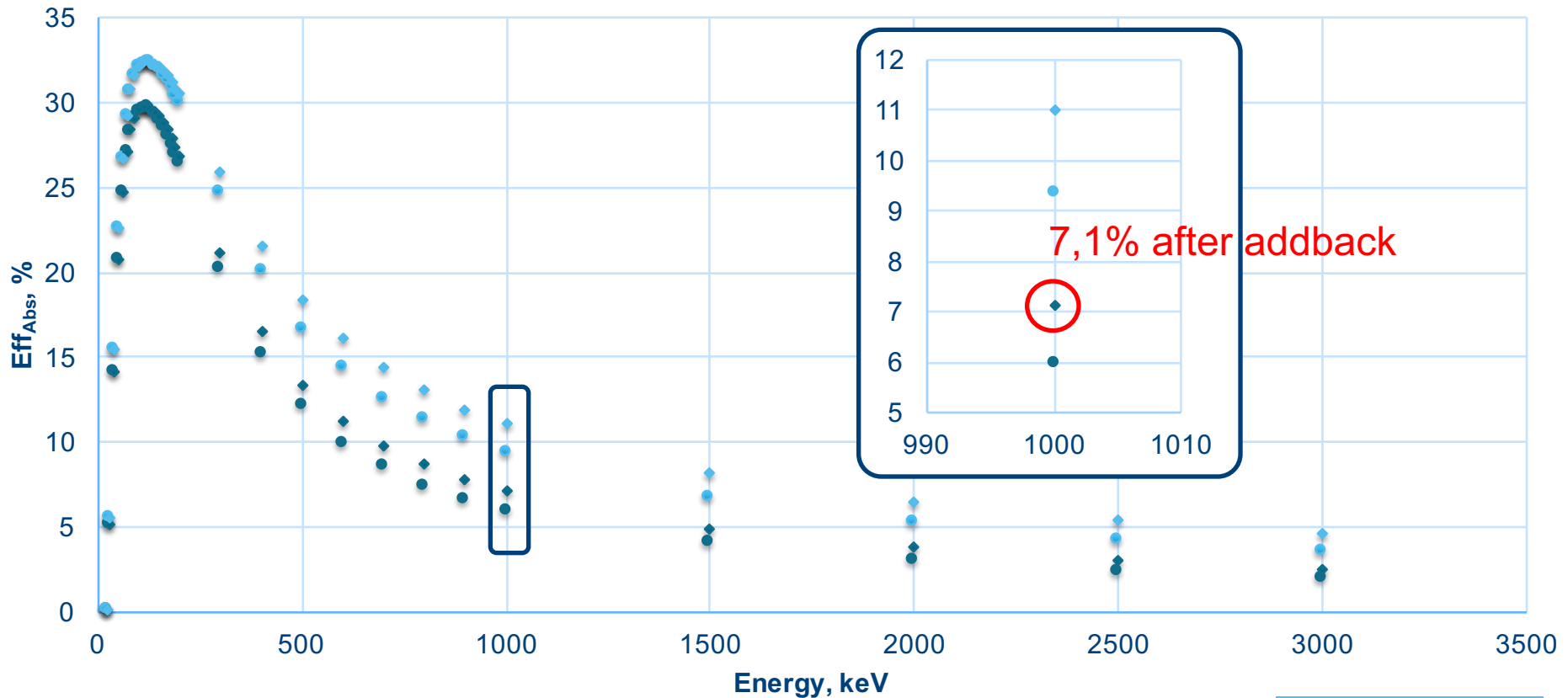
$$E_2 = 240 \text{ keV}$$

## Comparison of spectra before and after addback algorithm



## Comparison of $\text{Eff}_{\text{Abs}}$ before and after AddBack for $\text{CeBr}_3$ detector array

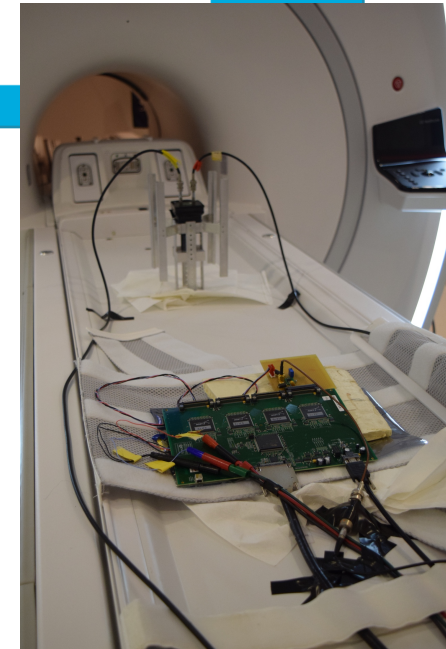
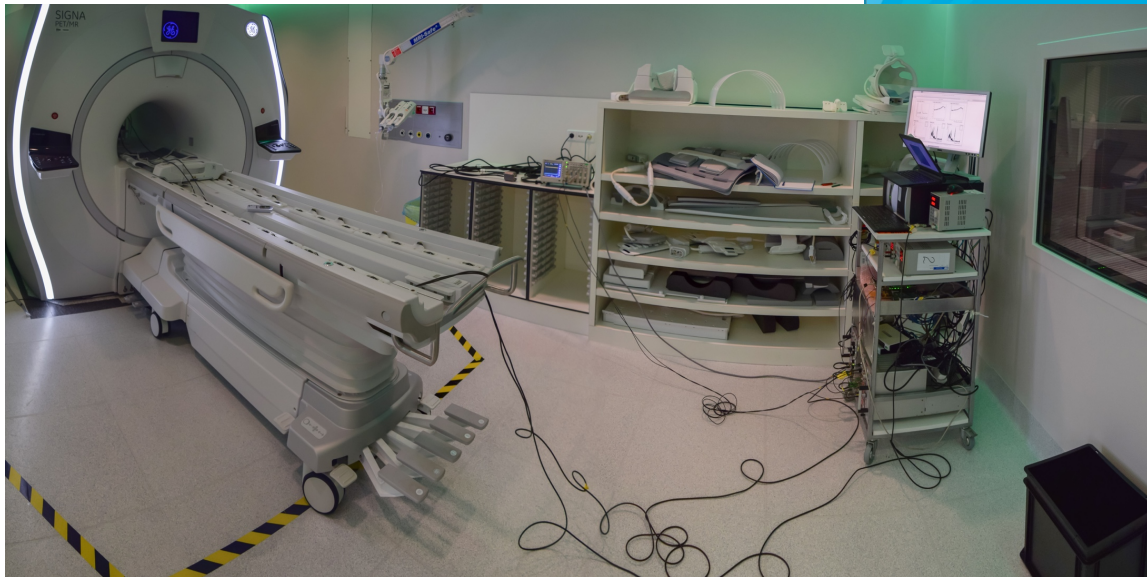
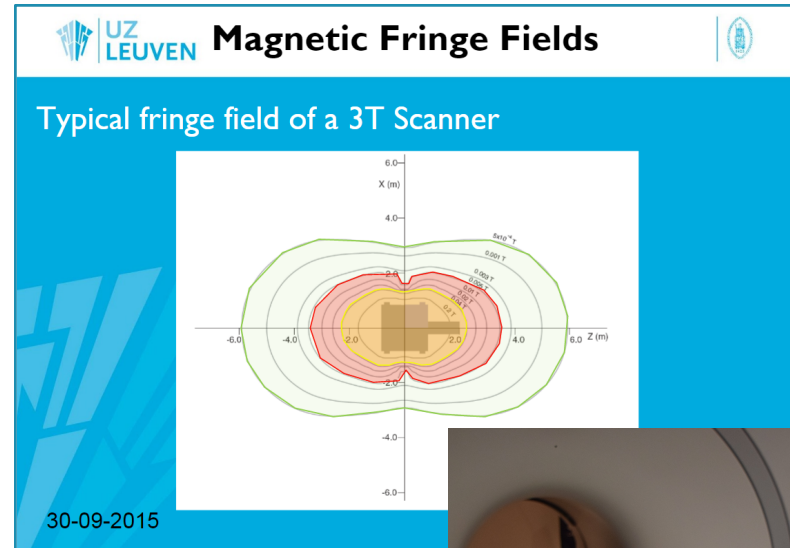
- Hex, 54cryst, 1,5"x1,5"x1,5", Rin=119,512mm
- Hex, 54cryst, 2"x2"x2", Rin=153,286mm
- ◆ Hex, 54cryst, 1,5"x1,5"x1,5", Rin=119,512mm, AddBack
- ◆ Hex, 54cryst, 2"x2"x2", Rin=153,286mm, AddBack



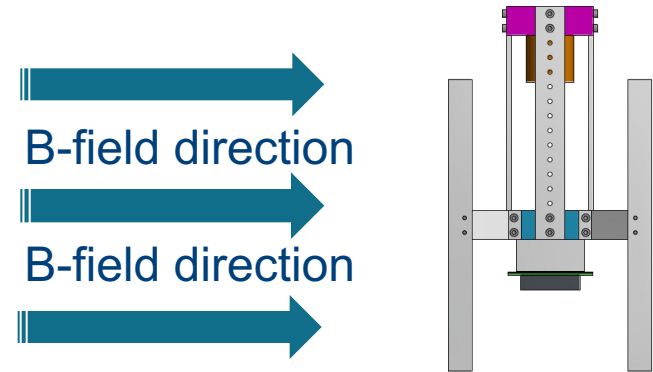
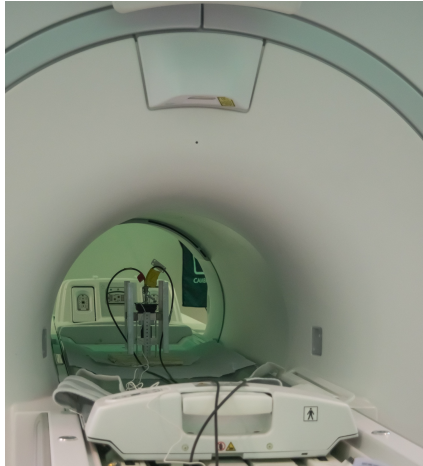
# Detector tests in 3T magnetic field @ UZ Leuven

## Description of the setup

- 1,5"x1,5"x1,5" cubic  $\text{LaBr}_3$  and  $\text{CeBr}_3$  crystals were coupled to C-series SiPM array and read out with **Analog, Standard digital (CAEN) and GET system**
- Superconducting magnet  
- B-field around 3T



# Detector tests in 3T magnetic field @ UZ Leuven



	DAQ	Analogue	CAEN	GET	GET
Detector	B-field	No field	No field	No field	AsAd in 3T
CeBr <sub>3</sub> +SiPM	No field	5,32±0,01%	5,66±0,01%	5,99±0,02%	6,49±0,02%
CeBr <sub>3</sub> +SiPM	3T	5,32±0,01%	5,63±0,01%	6,00±0,02%	
LaBr <sub>3</sub> +SiPM	No field	3,52±0,01%	3,73±0,01%	4,19±0,03%	
LaBr <sub>3</sub> +SiPM	3T	3,50±0,01%	3,91±0,01%	4,16±0,01%	

Resolution of the CeBr<sub>3</sub> and LaBr<sub>3</sub>:Ce detectors @ **661,7keV** coupled to 3 different DAQ systems in “no” magnetic field region (~0,001T) and in 3T magnetic field region.